

## 7. Soil-Mechanics Experiment

*J.K. Mitchell,<sup>a†</sup> L.G. Bromwell,<sup>b</sup> W.D. Carrier, III,<sup>c</sup> N.C. Costes,<sup>d</sup>  
W.N. Houston,<sup>a</sup> and R.F. Scott<sup>e</sup>*

### INTRODUCTION

The purpose of the soil-mechanics experiment is to obtain data on the physical characteristics and mechanical properties of the lunar soil at the surface and subsurface and the variations of these properties in lateral directions. The characteristics of the unconsolidated surface materials provide a record of the past influences of time, stress, and environment. Of particular importance are such properties as particle size and shape; particle-size distribution, density, strength, and compressibility; and the variations of these properties from point to point. An additional objective is to develop information that will aid in the interpretation of data obtained from other surface activities or experiments and in the development of lunar-surface models to aid in the solution of engineering properties associated with future lunar exploration.

The Apollo 15 soil-mechanics experiment has offered greater opportunity for study of the mechanical properties of the lunar soil than previous missions, not only because of the extended lunar-surface stay time and enhanced mobility provided by the lunar roving vehicle (Rover), but also because four new data sources were available for the first time. These sources were (1) the self-recording penetrometer (SRP), (2) new, larger diameter, thin-walled core tubes, (3) the Rover, and (4) the Apollo lunar-surface drill (ALSD). These data sources have provided the best bases for quantitative analyses thus far available in the Apollo Program.

For the first time, quantitative measurement of forces of interaction between a soil-testing device and the lunar surface has been possible. The diversity of the Hadley-Apennine area, the traverse capability provided by the Rover, and the extended extra-vehicular-activity (EVA) periods compared with the earlier missions have provided opportunity for study of the mechanical properties of the soil associated with several geologic units.

Although many of the analyses and results presented in this report are preliminary in nature and more detailed analyses and simulations are planned, the following main results have been obtained.

(1) Although the surface conditions appear quite similar throughout the Hadley-Apennine site, considerable variability exists in soil properties, both regionally and locally, as well as with depth.

(2) In situ densities range from approximately 1.36 to 2.15 g/cm<sup>3</sup>, a range that indicates very great ranges in strength and compressibility behavior.

(3) No evidence of deep-seated slope failures has been noted, although surficial downslope movement of soil has occurred, and the soil on steep slopes along the Apennine Front is in a near-failure condition.

(4) Quantitative data provided by the SRP and the soil-mechanics trench have indicated a density of almost 2 g/cm<sup>3</sup>, a friction angle of approximately 50°, and a cohesion of 1 kN/m<sup>2</sup> for the soil at station 8 (fig. 5-2, section 5). These values are higher than those deduced for sites studied in earlier missions.

(5) New core tubes developed for this mission performed very well, and subsequent studies should enable a reliable estimation of in situ densities from the returned samples.

These and a number of other conclusions have emerged from the data and analyses presented in this report.

---

<sup>a</sup>University of California at Berkeley.

<sup>b</sup>Massachusetts Institute of Technology.

<sup>c</sup>NASA Manned Spacecraft Center.

<sup>d</sup>NASA Marshall Space Flight Center.

<sup>e</sup>California Institute of Technology.

<sup>†</sup>Principal Investigator.

## SUMMARY OF PREVIOUS RESULTS

Observations at five Surveyor landing sites and at Mare Tranquillitatis (Apollo 11) and Oceanus Procellarum (Apollo 12) indicated relatively similar soil conditions, although Apollo 12 core-tube samples showed a greater variation in grain-size distribution with depth than had been found in the Apollo 11 core-tube samples. On the basis of data from these missions, it was established (refs. 7-1 and 7-2) that the lunar soil is generally composed of particles in the silty-fine-sand range and that the material possesses a small cohesion and a friction angle estimated to be  $35^\circ$  to  $40^\circ$ . Best estimates of the in-place density of the soil range from approximately 1.5 to 2.0 g/cm<sup>3</sup>. Simulation studies (ref. 7-3) have shown that both the cohesion and angle of internal friction are likely to be very sensitive functions of density.

Fra Mauro, the Apollo 14 landing site, represented a topographically and geologically different region of the Moon than had been visited previously. At that site, a greater variation in soil characteristics, both laterally and within the upper few tens of centimeters, was observed (ref. 7-4). Much coarser material (medium- to coarse-sand size) was encountered at depths of only a few centimeters at some points, and the soil, in some areas, was much less cohesive than the soil observed from previous missions. The results of measurements using the Apollo simple penetrometer suggested that the soil in the vicinity of the Apollo 14 Apollo lunar surface experiments package (ALSEP) may be somewhat stronger than soil at the landing sites of Surveyor III and VII as reported in reference 7-5. However, computations of soil cohesion at the site of the Apollo 14 soil-mechanics trench yield lower bound estimates (0.03 to 0.10 kN/m<sup>2</sup>) considerably less than anticipated (0.35 to 0.70 kN/cm<sup>2</sup>) from the results of earlier missions. Available data suggested also that the soil at the Fra Mauro site generally increases in strength with depth and is less dense and less strong at the rims of small craters than in level intercrater regions.

## METHODS

Quantitative analyses of the mechanical properties of the lunar soil in situ are made using two main approaches, singly and in combination. The approaches are (1) simulations, wherein terrestrial measurements are made using appropriately designed

lunar-soil simulants to provide a basis for prediction of probable behavior before the mission and replication of actual behavior after the mission and (2) theoretical analyses, which can be used to relate observed behavior to soil properties and imposed boundary conditions. Because of the difference between lunar and terrestrial gravity, theoretical adjustment of the results of simulations usually is required.

Houston and Namiq (ref. 7-6) and Costes et al. (ref. 7-7) have described simulation studies for the prediction of the penetration resistance of lunar soils and the evaluation of lunar-soil mechanical properties from in-place penetration data. Mitchell et al. (ref. 7-3) relate footprint depth to soil density. Houston and Mitchell (ref. 7-8) and Carrier et al. (ref. 7-9) describe how simulations can be used to determine the influences of core-tube sampling on the original properties of the lunar soil.

Theories of soil mechanics are reasonably well established, although the inherent variability of most soils and difficulties in determination of stresses in the ground require judgment in the application of these theories. Scott (ref. 7-10) and other soil-mechanics texts present these theories in detail. The theory of elasticity is used for computation of stresses and displacements, and the theory of plasticity is used to relate failure stresses and loads to soil-strength parameters. For these failure analyses, the Mohr-Coulomb strength theory is used. According to this theory, which has been shown to be sufficiently accurate for most terrestrial soils, the shear strength  $s$  can be represented by

$$s = c + \sigma \tan \phi \quad (7-1)$$

where  $c$  is unit cohesion,  $\sigma$  is normal stress on the failure plane, and  $\phi$  is the angle of internal friction. It has been assumed, on the basis of extremely limited laboratory data, that the same approach can be applied to lunar-soil behavior.

## DESCRIPTION OF DATA SOURCES

As has been the case for the three previous Apollo missions, observational data provided by crew commentary and debriefings and by photography have been useful for deduction of soil properties. The excellent quality of the television, coupled with the fact that video coverage was available for most of the stations visited by the crew, has made detailed study

of some of the activities of interest to the soil-mechanics experiment possible. Interactions between the astronauts and the lunar surface, as indicated by their footprints, and interactions of the small scoop, tongs, core tubes, and flagpole with the lunar surface, have provided valuable soil-behavior information. Quantitative data have been obtained from the following sources.

### Soil-Mechanics Trench

During EVA-2, the lunar module pilot (LMP) excavated a trench at station 8 (fig. 5-2, section 5) with a near-vertical face to a depth of approximately 28 cm. This trench provides data on soil conditions with depth and a basis for computation of soil cohesion, as described subsequently in this section.

### Self-Recording Penetrometer

The SRP, available for the first time on Apollo 15, was used to obtain data on penetration compared to force in the upper part of the lunar soil. The SRP (fig. 7-1) weighs 2.3 kg, can penetrate to a maximum depth of 76 cm, and can measure penetration force to a maximum of 111 N. The record of each penetration is scribed on a recording drum contained in the upper housing assembly.

The lunar-surface reference plane, which folds for storage, rests on the lunar surface during a measurement and serves as datum for measurement of penetration depth. Three penetrating cones, each of 30° apex angle and base areas of 1.29, 3.22, and 6.45

cm<sup>2</sup>, are available for attachment to the penetration shaft, as well as a 2.54- by 12.7-cm bearing plate. The 3.22-cm<sup>2</sup> (base area) cone and the bearing plate were used for a series of six measurements at station 8. The SRP is shown in use during a premission simulation at the NASA Kennedy Space Center in figure 7-2.

### Core Tubes

Core tubes of a different design than those previously available were used during the Apollo 15 mission. These thin-walled tubes made of aluminum are 37.5 cm long, 4.13 cm inside diameter, and 4.38 cm outside diameter. Individual tubes can be used singly or in combination. The components of a double-core-tube assembly are shown in figure 7-3; a double-core-tube sampling at station 9A during EVA-3 is depicted in figure 7-4.

The new core-tube designs were developed to satisfy three objectives: (1) to reduce the amount of sample disturbance, (2) to increase the size of the sample, and (3) to facilitate ease of sampling by the crew. These considerations are discussed in references 7-8 and 7-9. Preliminary evaluations based on crew comments and on Lunar Sample Preliminary Examination Team (LSPET) examination of the Apollo 15 cores indicate that these objectives were achieved.

### Rover

The Rover is a four-wheeled surface vehicle with a double-Ackerman steering system. Each wheel is powered by an electric motor. The wheel "tires" are

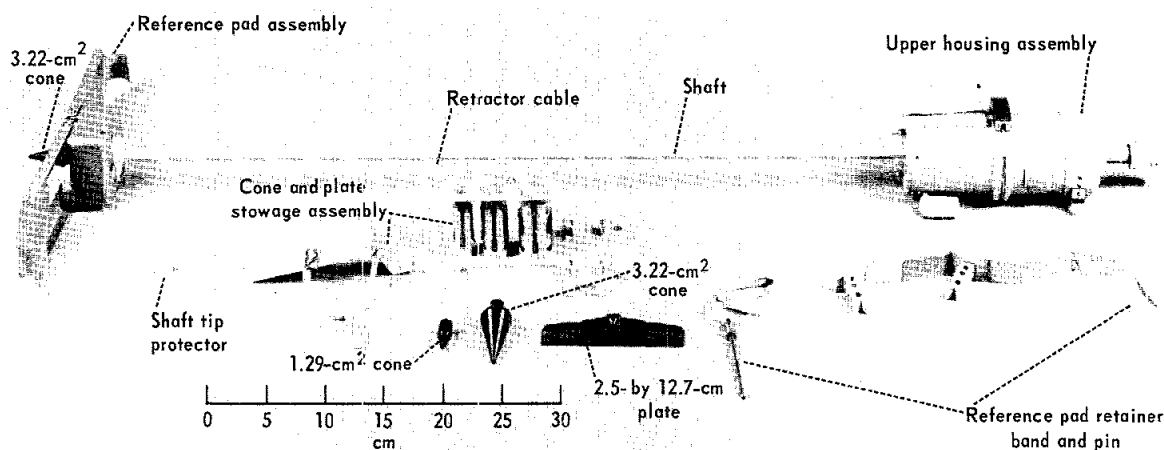


FIGURE 7-1.—Self-recording penetrometer.



FIGURE 7-2.—Self-recording penetrometer in use during premission simulation.

approximately 290 N. At this load, the average unit pressure exerted by the wheel on the soil is approximately  $0.7 \text{ N/cm}^2$  and the tire deflection is 5.1 cm. At wheel loads of 178 N and 377 N, corresponding to wheel-load transfer at slope angles of  $20^\circ$ , the wheel deflections are 3.6 cm and 5.6 cm, respectively. The Rover is shown in the vicinity of the ALSEP site during EVA-1 in figure 7-5.

### SOIL CHARACTERISTICS AT THE HADLEY-APENNINE SITE

Soil cover is present at all points in the Hadley-Apennine Region except for the bedrock exposures visible on the Hadley Rille wall. The soil layer appears to become thinner going down over the rim of the rille. Away from the rille, a soil depth of 3 to 4.5 m was estimated by the commander (CDR) on the basis of a crater observed during EVA-2. The surface appears similar in color (i.e., shades of gray and gray-brown) to that seen at the other Apollo sites, although wider variations were observed. Surface textures are also similar, ranging from smooth areas free of rock fragments through patterned ground to

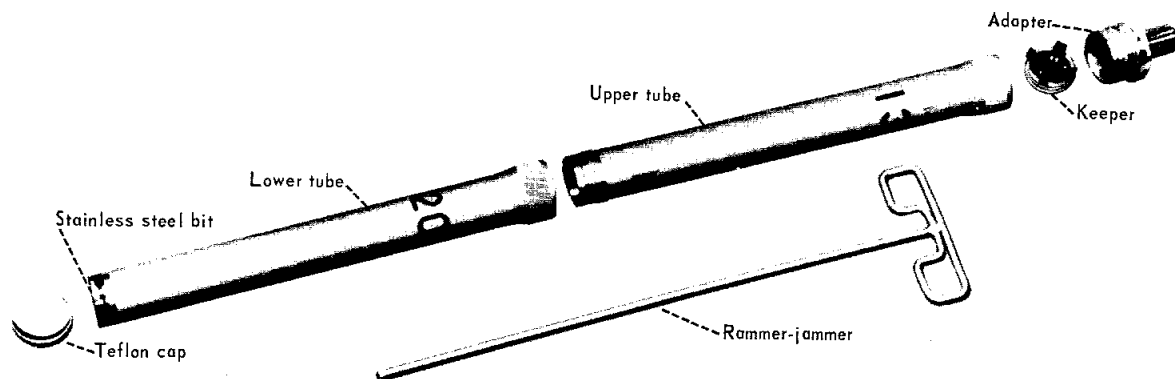


FIGURE 7-3.—Apollo 15 double core tube as used on EVA-1 and EVA-3. The single tube taken on EVA-2 was an upper tube.

made of thin, steel, piano-wire mesh, and 50 percent of the contact area with the lunar surface is covered with a chevron tread. The unloaded wheel has a diameter of 81.5 cm, a section width of 23.2 cm, and a section height of 18.6 cm. The average wheel load on level ground in lunar gravity, including the weight of the vehicle, the payload, and two crewmen, is

areas heavily populated by larger rocks and fragments. Of considerable interest and importance is the fact that the soil strength and compressibility (and, therefore, almost certainly, the density) vary significantly, not only on a large scale from station to station but also locally within short distances, as will be shown later.



FIGURE 7-4.—Double core tube at station 9A pushed to a depth of 22 cm. The tube was driven to a final depth of 68 cm by application of approximately 50 hammer blows (AS15-82-11161).

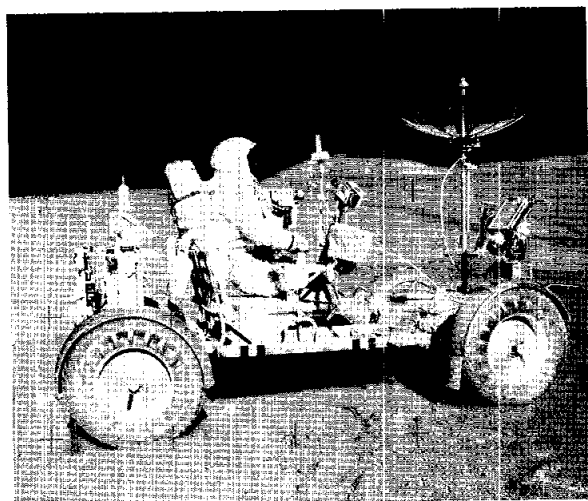


FIGURE 7-5.—Rover near ALSEP site during EVA-1 (AS15-85-11471).

### Textural and Compositional Characteristics

Grain-size-distribution curves have been obtained by the LSPET for samples from several locations. Some are shown in figure 7-6, and bands indicating size ranges for samples from the previous Apollo sites (refs. 7-11 and 7-12) are also indicated. It is of interest that the samples examined thus far do not exhibit as much variability in grain-size distribution as that observed for different samples from the Apollo 12 and 14 sites. Available distributions indicate the

Apollo 15 soils to be well-graded, silty, fine sands and fine, sandy silts. The sample from bag 194 (station 7 near Spur Crater) is one of the coarsest samples returned. No data are available on size distributions of particles finer than 0.044 mm. Photomicrographs of four size ranges from a sample taken at the bottom of the soil-mechanics trench are shown in figure 7-7. It may be seen that most particles are subrounded to angular, with occasional spherical particles. Gross particle shapes are typical of those in terrestrial soils of similar gradations. However, the surface textures of many of the particles (e.g., the agglutinates and the microbreccias) are more irregular than in common terrestrial soils. The influences of these unusual characteristics on mechanical properties are yet to be determined.

Study of the soil fraction finer than 1 mm by the LSPET has shown that soils from different areas have different compositions (table 7-I). It is reasonable to expect that some of the physical-property differences observed in different areas reflect these compositional differences.

### Soil Profiles

Data on the variability of lunar-soil properties with depth below the surface are available from four sources: the core tubes, the deep core sample obtained using the ALSD, the soil-mechanics trench, and the SRP. The LMP reported no signs of layering while excavating the trench to a depth of 30 cm at station 8, and no layering is visible in the photographs of the trench. However, the LMP did report encountering some small white and black fragments. The trench bottom was reported to be of much firmer material than the overlying soil. Samples from the trench bottom were chipped out in platy fragments approximately 0.5 cm in length.

However, the results of X-ray examination of the core tubes and deep drill samples have led the LSPET to conclude that many different units exist with depth. The presence of a large number of units indicates a very complex soil structure, which implies a high local variability in properties.

### Core Samples

*Drive tubes.*—More than three times as much lunar soil and rock was returned in the Apollo 15 drive core tubes than from the three previous missions com-

## APOLLO 15 PRELIMINARY SCIENCE REPORT

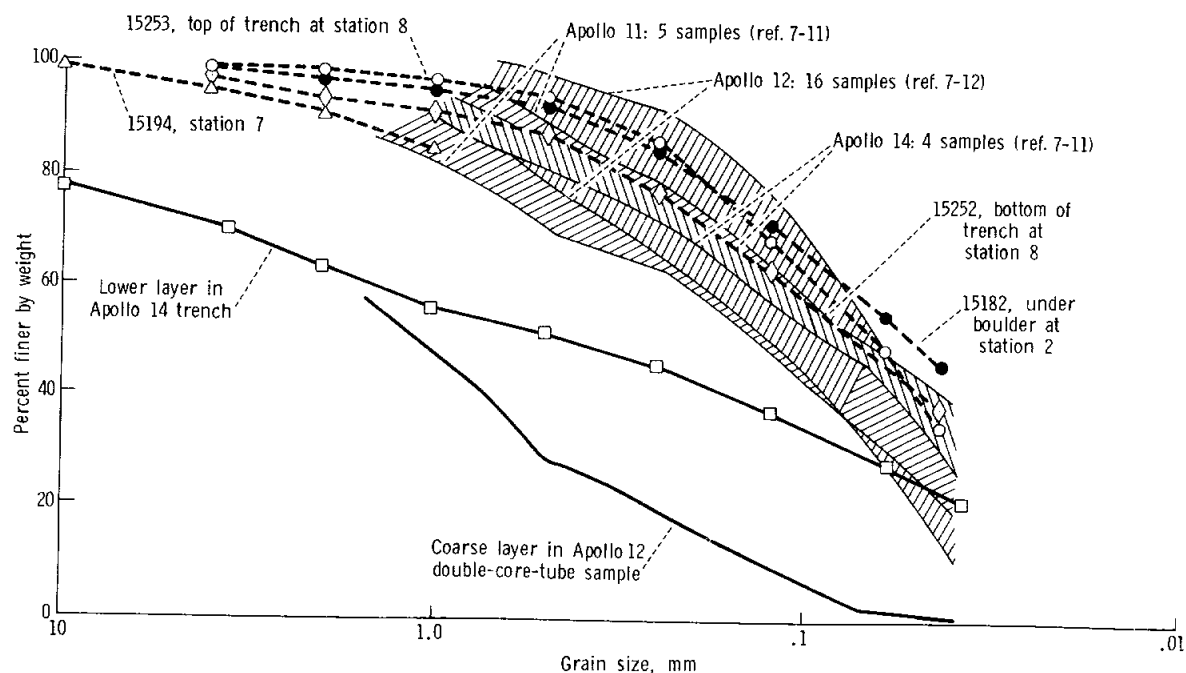


FIGURE 7-6.—Grain-size-distribution curves for several Apollo 15 samples compared with curves for samples from other Apollo sites.

bined (3302 g compared to 932 g). The core samples also appear to be less disturbed than the earlier samples. These improvements are a direct result of a new core tube designed on the basis of soil-mechanics considerations. The new tubes (fig. 7-3) reflect four important changes compared with the tubes designed for use in the previous missions: (1) inside diameter increased from 1.97 to 4.13 cm (the geometry of the Apollo 11, 12 to 14, and 15 core tubes are compared in fig. 7-8), (2) decreased wall thickness, (3) elimination of the Teflon follower and the introduction of the keeper, and (4) redesign of the bit.

The previous core tubes used a follower that was pushed up inside the core tube by the soil column during sampling. The follower was intended to resist movement of the soil inside the tube until it could be returned to Earth. Unfortunately, the follower also exerted a force of approximately 13 N to the soil during sampling, which adversely affected the recovery ratio.<sup>1</sup> Simulations performed by Carrier et al. (ref. 7-9) indicated that the follower reduced the recovery ratio from 80 percent to 55 percent for an

Apollo 12 to 14 single-core-tube sample and from 70 percent to 63 percent for a double-core-tube sample. The new keeper, shown in the exploded view of the Apollo 15 core tube in figure 7-3, is stored in the adapter until after the sample has been obtained. The astronaut then inserts the "rammer-jammer" through a hole in the top of the adapter and pushes the keeper down until it comes into contact with the soil. The keeper has four leaf springs that dig into the wall of the core tube and resist movement in the opposite direction, thereby containing and preserving the core sample.

*Drive core samples.*—One core-tube sample was recovered on each of the Apollo 15 EVA periods. Data for these samples are given in table 7-II. A double-core-tube sample was taken at station 2 (fig. 5-2, section 5) on the rim of a 10-m crater between Elbow and St. George Craters at the Apennine Front. The crew pushed the first tube to the full depth, and 35 hammer blows were required to sink the upper tube. A single core was taken at station 6 inside the rim of a 10-m crater, approximately 500 m east of Spur Crater, also at the Apennine Front. The tube was pushed to full depth and no hammering was necessary. A double-core-tube sample was recovered at station 9A at the edge of Hadley Rille, approxi-

<sup>1</sup> Ratio of length of sample obtained to depth tube driven  $\times 100$  percent.

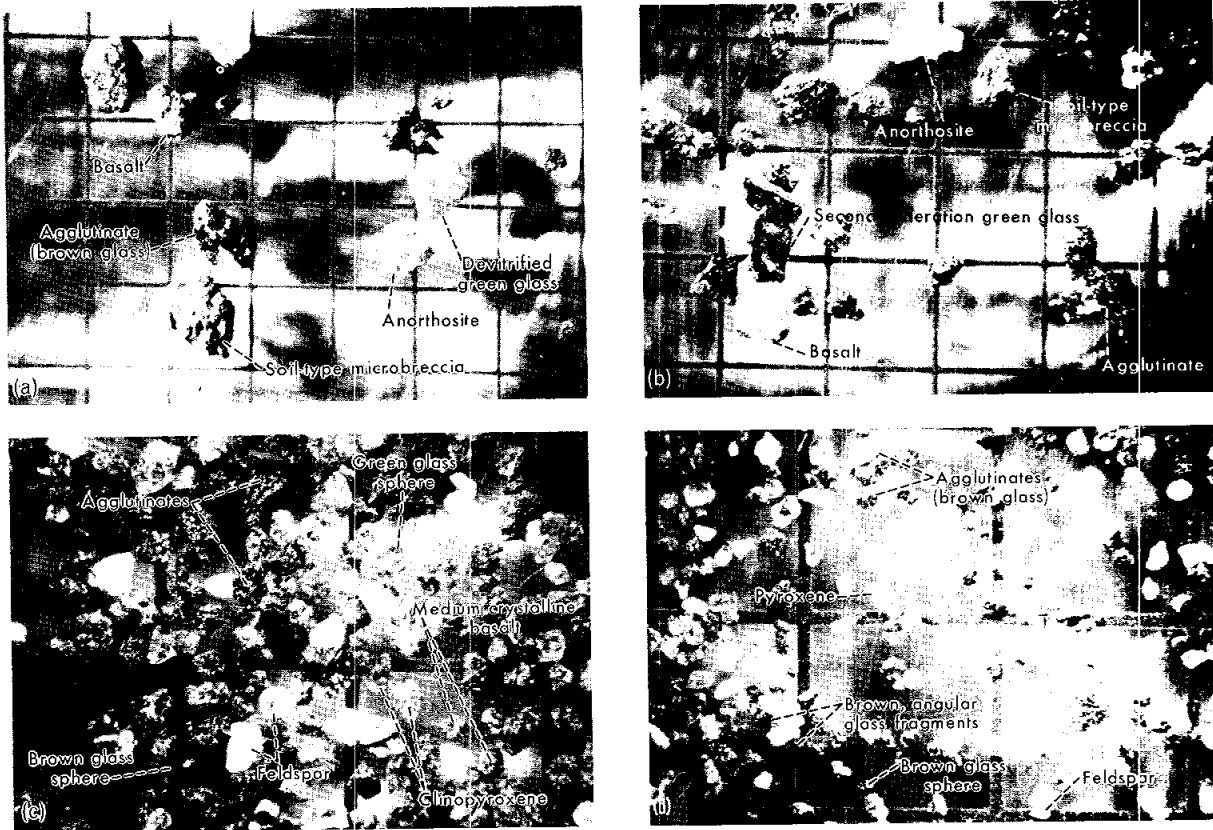


FIGURE 7-7.—Photomicrographs of four particle-size ranges from sample taken at the bottom of the soil-mechanics trench. Grid lines in photographs are 1 by 1 mm. (a) 0.5 to 1 mm (S-71-45452). (b) 0.25 to 0.5 mm (S-71-45446). (c) 0.125 to 0.25 mm (S-71-45450). (d) 0.0625 to 0.125 mm (S-71-45444).

TABLE 7-1.—*Compositional Characteristics of Different Soil Samples<sup>a</sup>*

Type of material	Composition, percent, at —				
	Apennine Front area			Lunar module area	Hadley Rille area
	Station 2	Station 6	Station 7		Station 9
Agglutinates and brown glass	~25	~46	~18	High	16 to 35
Clear green glass	12	4 to 6	High	None	<2
Mafic silicates	~18	10 to 20		15 to 20	10 to 30
Feldspar	30 to 40	18 to 20	16	6 to 10	20 to 35
Anorthosite		0 to 10	5 to 8	4 to 10	
Microbreccia		5 to 30		Trace	
Crystalline basalt			5 to 8	5 to 6	5 to 25

<sup>a</sup>Determined by the Lunar Sample Preliminary Examination Team.

mately 200 m west of Scarp Crater. The crew was able to push the tube to a depth of only two-thirds of the length of the bottom tube, and approximately 50 hammer blows were required to drive the tube to full

depth. This additional driving effort was undoubtedly attributable to a higher soil density and strength at this location (as discussed later) as well as to the presence of rock fragments in the soil matrix.

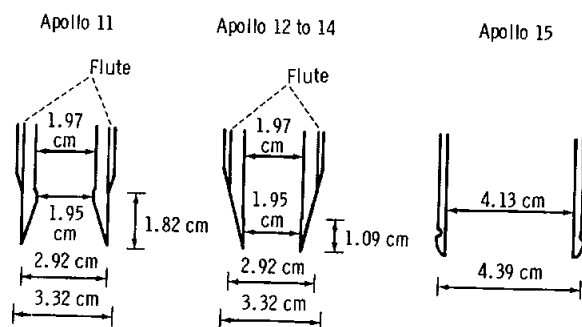


FIGURE 7-8.—Comparison of core-tube-bit designs for different Apollo missions.

To date, the core tubes have only been weighed and X-rayed in the Lunar Receiving Laboratory (LRL). A detailed description of the core samples on the basis of these X-radiographs is presented in section 6. Considerable stratigraphy has been observed as noted earlier, and careful study of the drive-tube samples should be most enlightening.

The X-radiographs also permit the determination of the core-sample lengths and the bulk densities,

which are also presented in table 7-II. In the lower half of the sample from station 2, the sample length was found to be slightly less than nominal. This discovery would indicate either that the sample fell out of the top when the two halves were unscrewed or that the sample was compressed slightly when the keeper was inserted.

In the single core tube, the keeper was found to have remained in the stowed location in the adapter. Because the crew inserted the rammer-jammer properly, it has been concluded that the keeper slipped back up the tube. The result was that the sample expanded to a length of 36.2 cm, corresponding to a bulk density of 1.28 g/cm<sup>3</sup>. If a nominal length of 34.9 cm is used, the calculated bulk density is 1.33 g/cm<sup>3</sup>. In addition, the X-radiographs reveal a void along one side at the bottom of this tube. The crew described this sample location as having a coarser grain-size distribution than at other points at station 6, and this situation may account for part of the sample falling out of the tube before it was capped. The void was estimated to occupy 6 cm<sup>3</sup> (less than 2 percent of the total volume), and the bulk density

TABLE 7-II.—Preliminary Data on Apollo 15 Core Samples

Serial no.	Sample no.	Station	Weight, g	Length, cm	Bulk density, g/cm <sup>3</sup>	Tube depth (pushed), cm	Total depth (pushed and driven), cm	Hammer blows, no.	Core recovery, percent
Drive tube (4.13 cm inside diameter)									
EVA-1 <sup>a</sup> 2003	15008	2	510.1	28 ± 1	1.36 ± 0.05	34.6	70.1	35	88 to 93
<sup>a</sup> 2010	15007		768.7	<sup>b</sup> 33.9 to 34.9	1.64 to 1.69				
EVA-2	15009	6	622.0	<sup>c</sup> 36.2 to 34.9	1.35	34.6	34.6	0	101 to 105
EVA-3	15011	9A	660.7	29.2 ± 0.5	1.69 ± 0.03	22.4	67.6	~50	91 to 96
<sup>a</sup> 2009	15010		740.4	<sup>b</sup> 32.9 to 34.9	1.79 to 1.91				
<sup>a</sup> 2014									
Drill stem (2.04 cm inside diameter)									
022 (top)	15006	8	210.6	32.9 to 39.9	1.62 to 1.96	<sup>d</sup> ~236	--	--	100 to 102
023	15005		239.1	39.9	1.84				
011	15004		227.9	39.9	1.75				
020	15003		223.0	39.9	1.79				
010	15002		210.1	39.9	1.62				
027 (bottom)	15001		232.8	<sup>e</sup> 33.2 ± 0.5 by 42.5	2.15 ± 0.03				

<sup>a</sup>Double.

<sup>b</sup>Sample either fell out of top of lower half of tube or was compressed when keeper was inserted.

<sup>c</sup>Nominal length is 34.9 cm; keeper slipped out of position.

<sup>d</sup>Drilled full depth.

<sup>e</sup>Sample fell out of the bottom of the drill stem.



was corrected to  $1.35 \text{ g/cm}^3$  accordingly. This density and that of the top half of the double-core-tube sample from station 2 are approximately 15 percent lower than the density of any of the samples previously returned.

As determined from the X-radiograph of the returned sample tube, approximately  $54 \text{ cm}^3$  of soil fell out of the bottom of the tube taken at station 9A before the tube was capped. In addition, the sample length was found to be less than nominal. This discovery would indicate either that the sample fell out of the top when the two halves were unscrewed or that the sample was compressed when the keeper was inserted. The high relative density at this location contradicts the latter interpretation and supports the former. Until further studies can be made, a range of possible densities is indicated as shown in table 7-II.

*Drill-stem samples.*—Characteristics of the ALSD and the deep drill-sampling procedure are described in section 11. The sample lengths shown in table 7-II were determined from X-radiographs that are discussed in detail in section 6. The sample length for the top section (serial number 022) was difficult to determine accurately, and a range of values is indicated. Some of the core (approximately 9.3 cm) fell out of the bottom of the drill stem (serial number 027). The bulk density of the remaining portion is approximately  $2.15 \text{ g/cm}^3$ , which is 8 percent higher than the density of any previously returned core sample.

### Soil Variability

One of the most striking characteristics of the soils in the Hadley-Apennine region is the great variability in properties from point to point, both regionally and locally. Vertical variability is indicated by the different units and densities observed in the core samples.

A series of footprints from different stations is shown in figure 7-9. In general, the deeper the footprint, the less dense, less strong, and more compressible the soil. Simulations (ref. 7-3) have shown that only small differences in the depth of footprints correspond to relatively large differences in soil properties. On the average, the soil on the Front was less strong and less dense than that by the lunar module (LM) and at the ALSEP site, and the surface was free of significant numbers of large fragments. In general, near Hadley Rille, the soil was relatively strong and less compressible than in other areas. Large fragments were abundant on the surface. The

holes remaining after core-tube sampling at stations 6 and 9A are shown in figure 7-10. Bulging of the ground surface around the hole at station 9A indicates a stronger, less compressible soil than at station 6. As noted earlier, the single core tube at station 6 was pushed easily to the full depth, whereas the bottom tube of the double core at station 9A could be pushed only to two-thirds of the depth. These findings were somewhat surprising, because pre-mission expectations had been that the Apennine Front would be firm with abundant coarse fragments and that the maria areas would be soft.

Local variations in strength and compressibility are common as well; an example of these variations in the vicinity of the LM is shown in figure 7-11. Footprints several centimeters deep may be seen in the foreground, whereas very little sinkage is seen in the middle ground area of the photograph.

### Dust and Adhesion

Numerous instances of dust adherence to equipment, astronauts' suits, and lunar rocks were reported during the Apollo 15 EVA periods. The quantity of dust adhering to objects and the number of instances where brushing and cleaning were necessary were much more frequent than on previous missions, with the possible exception of the Apollo 12 mission.

The Rover kicked up quantities of dust during acceleration and when passing through the rims of soft craters. Little of the dust impacted on the Rover itself or on the astronauts, and it did not cause any problems with visibility or operation of the vehicle, although frequent cleaning of the lunar communications relay unit (LCRU) was required to prevent overheating of the television camera circuits. No dust accumulation was noted in the wire wheels, but a thin layer of dust eventually covered most of the vehicle.

Minor operational problems were caused by thin layers of dust on the camera lenses and dials, gnomon color chart, navigation maps, and LCRU mirror. As on previous missions, the adhering dust was brushed off easily. However, the dust was so prevalent that, during part of the mission, the astronauts reported that, to set the lens, dust had to be wiped from the camera settings every time they took a picture.

### SLOPE STABILITY

A preliminary study of the 70- and 500-mm

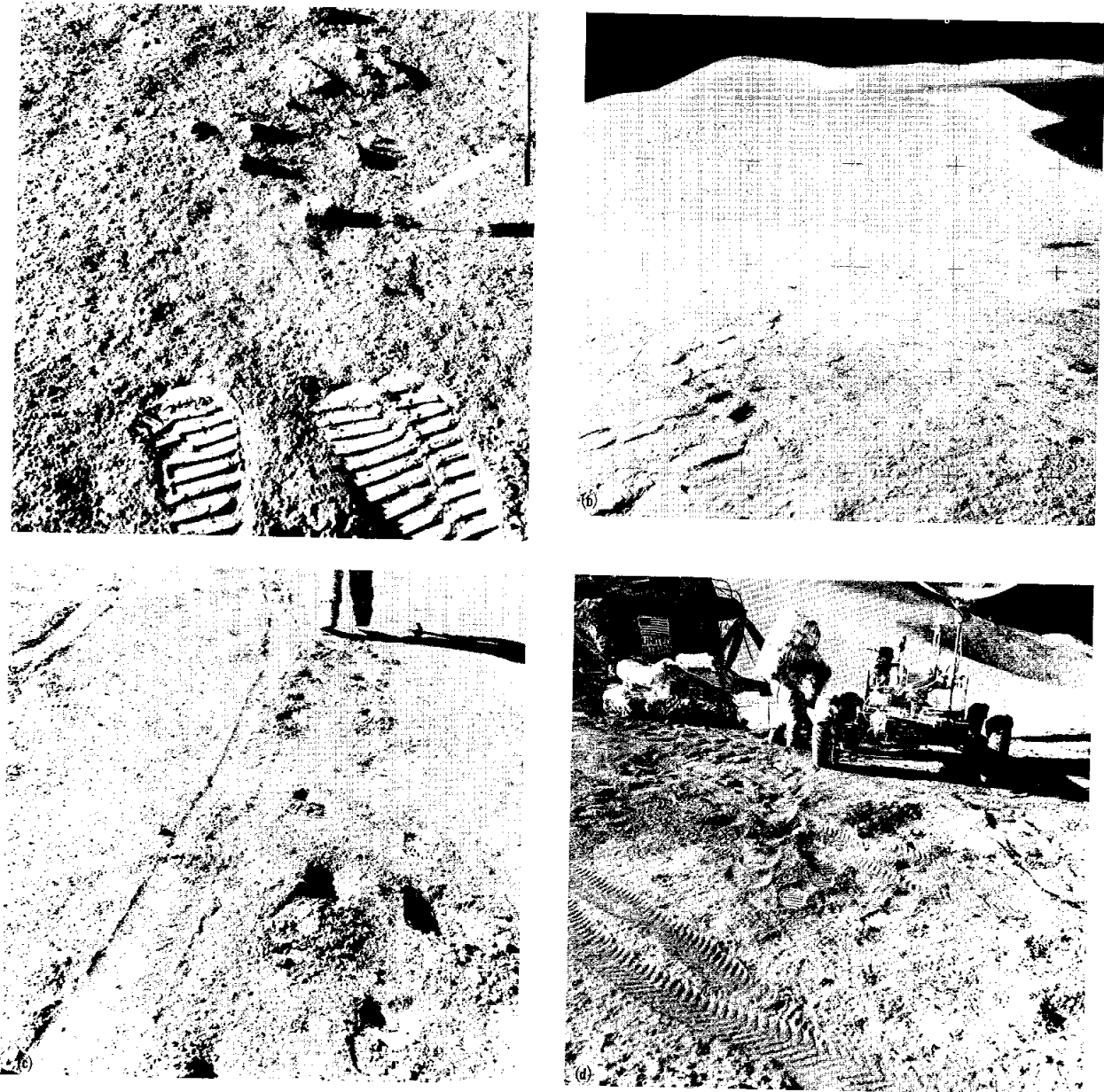


FIGURE 7-9.—Footprints from several locations illustrating soils of different strength. (a) Moderately firm soil at station 1 (AS15-86-11534). (b) Soft soil at station 2 (AS15-85-11424). (c) Very soft to soft soil at station 6 (AS15-86-11654). (d) Medium-strong soil at the LM (AS15-86-11599).

photography available thus far has been made for evidence of slope instability and past slope failures. No indications exist of previous deep-seated slope failures of the type that have been suggested by Lunar Orbiter photos of some areas of the Moon.

The near-surface zones of some slopes may be near

incipient failure, however. The foreground of figure 7-12 shows failure under footprints as one of the astronauts traversed the slope in the vicinity of station 6A. Detailed analysis of conditions in this area must await more precise determination of the slope angle, which is estimated to be  $10^{\circ}$  to  $20^{\circ}$ .

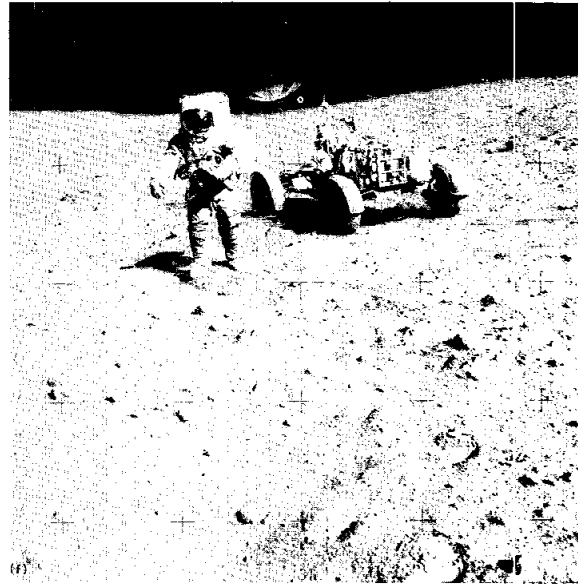
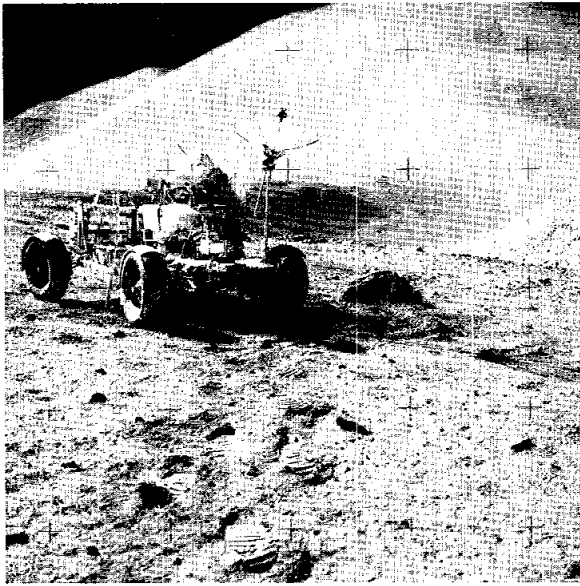


FIGURE 7-9.—Concluded. (e) Moderately firm to firm soil at station 9A (AS15-82-11121). (f) Firm soil at station 10 (AS15-82-11168).



FIGURE 7-10.—Core-tube holes at two sampling sites. (a) Core-tube hole at station 6 (AS15-86-11651). (b) Core-tube hole at station 9A. The raised ground surface around the station 9A hole indicates stronger, less compressible soil than at station 6 (AS15-82-11163).

Downslope movement of surficial material on the rille walls is evident. The movement of fine-grained material has left bedrock exposed on the upper slopes in some areas. Fillets are seen on the uphill side of many rocks, indicating soil movement around the rock. Other rocks without fillets can be seen, which suggests that (1) the rock itself may have rolled or slid downhill relative to the soil or (2) the soil in the

vicinity of the rock has not undergone movement. Because no boulder tracks are visible, any rock movements must have occurred sufficiently long ago for subsequent soil movement to fill in any tracks formed initially. But if tracks have been filled in, then the associated rocks would be expected to be filleted as a result of the soil movement. Thus, the second hypothesis appears to be more tenable.



FIGURE 7-11.—Local variability in soil strength and density as indicated by shallow and deep footprints in the vicinity of the LM (AS15-92-12445).

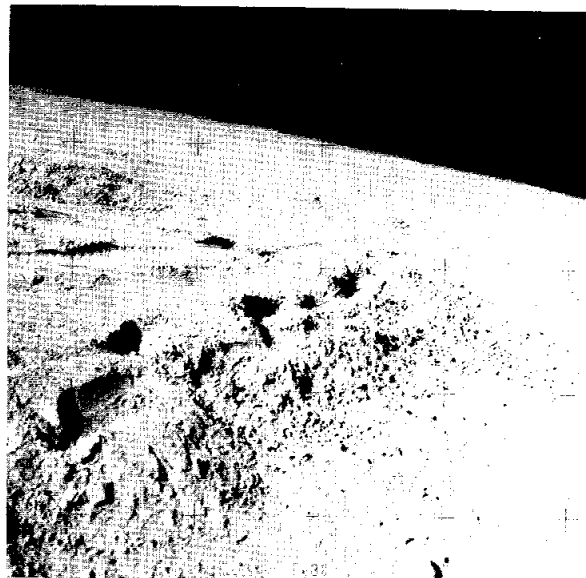


FIGURE 7-12.—Incipient slope failure as indicated by slipping out of soil beneath astronauts' feet (AS15-90-12197).

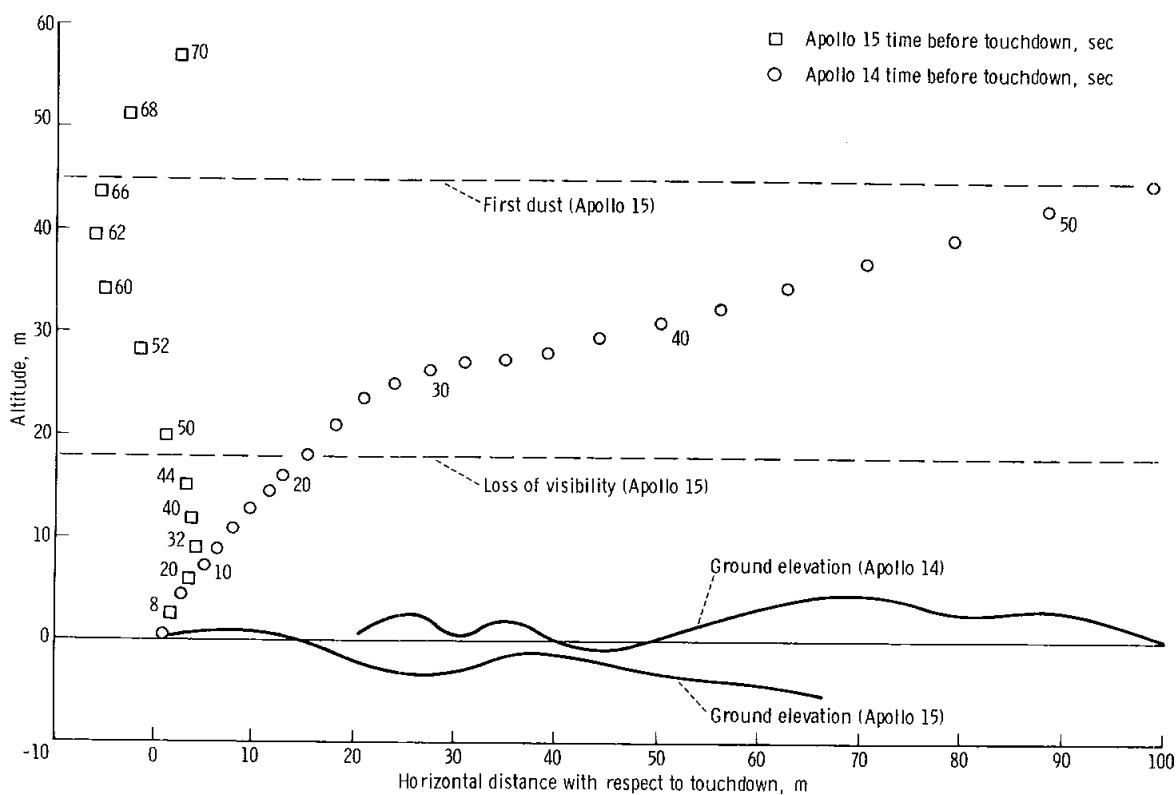


FIGURE 7-13.—Apollo 14 and Apollo 15 descent trajectories.

## SOIL BEHAVIOR DURING LM DESCENT AND LANDING

The Apollo 15 descent was much steeper and considerably slower than those of previous Apollo landings. The Apollo 14 and 15 descent trajectories are compared in figure 7-13. The final 30 m of descent occurred essentially vertically in a period of approximately 60 sec. In earlier landings (refs. 7-1, 7-2, and 7-4), only the last 3 to 6 m of descent were more or less vertical and occupied about half the time required for the Apollo 15 LM to descend through the same distance. The crew commented that they observed the first lunar-surface dust movement resulting from their landing at a height of approximately 46 m and noted that the last 18 m of descent were accomplished under conditions of no surface visibility as a result of the quantity of lunar soil being eroded by the descent engine. These were, therefore, the poorest visibility conditions during any Apollo landing. Previously, blowing dust had caused major difficulties only in the Apollo 12 descent and then only in the final 6 m. The dust problem may be related to the nature of the descent path and vertical velocity as well as to the local soil and the Sun-angle conditions.

Once again, from the photographs of the landing gear taken on the lunar surface, no stroking of the shock absorbers is evident, indicating only small, dynamic impact forces during landing. Only nominal penetration of the footpads into the lunar surface to a depth of several centimeters has occurred. However, in the landed position (fig. 7-14), the LM is tilted up to the west approximately  $8^\circ$  and up to the north through the same angle because of the lunar-surface topography. The +Z and +Y footpads appear to have landed on a slight rise, whereas the -Z footpad rests in a shallow crater 5 or 6 m in diameter. The -Y footpad is also in a slight depression. The LM is oriented with the +Z axis (the leg with the ladder) pointing due west. In the landing, principally as a consequence of the topographic relief, the descent-engine bell contacted the surface, crushing the bell slightly. The Apollo 15 mission is the first on which this has occurred and may have resulted, in part, from the fact that the Apollo 15 LM engine bell is larger than those used in earlier missions. No photographic indications are visible showing any lateral translation of the footpads during the final stages of descent. Because the underside of the LM so closely ap-

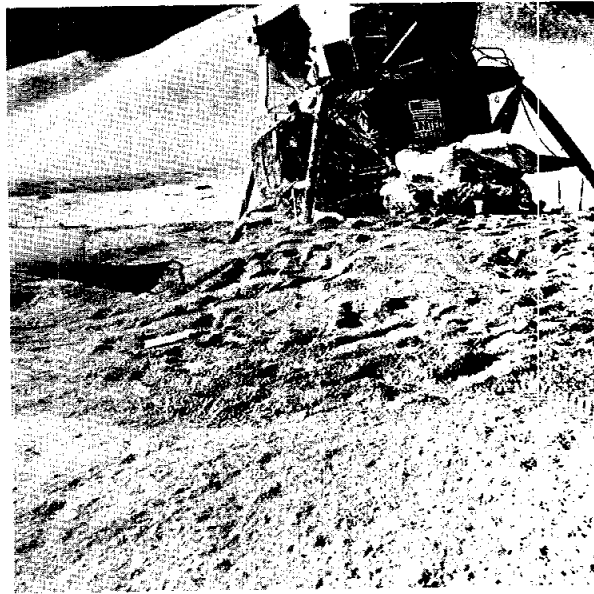


FIGURE 7-14.—The LM in the landed position is tilted up approximately  $8^\circ$  to the northwest because of surface topography (AS15-86-11600).

proached the lunar surface, the surface area below the spacecraft is largely in shadow, and signs of the erosion that took place in descent are not evident. In addition, on this mission, the photographs of the area around the landed LM were not taken soon enough after landing to show the surface undisturbed by the astronauts' surface operations. On photograph AS15-85-11364, taken from the top of the LM before astronaut egress, some signs of possible erosion tracks across the surface can be seen.

## SOIL-ROVER INTERACTION

The use of Rover-performance data and the interaction of the Rover wheels with the lunar surface as indicators of variability in the consistency and mechanical properties of the surficial material in the Hadley-Apennine region can be made in several ways, including the following.

- (1) Differences in the mean depth, shape, and surface texture of tracks developed by the chevron-covered Rover wire-mesh wheels

- (2) Extent and shape of a "rooster tail," developed by fine-grained material ejected as a result of wheel-soil interaction, and characteristic speeds at which such a rooster tail is developed or astronaut visibility is degraded (or both)

(3) Net accumulation of fine-grained material inside the open wire-mesh wheel

(4) Variations in mobility performance or power consumption under constant throttle for a given slope and surface roughness

(5) Variations in the ability of the vehicle to climb slopes of the same inclination

(6) Vehicle immobilization resulting from wheel spin-out or skidding at different areas

No quantitative information exists regarding the interaction of the Rover with the lunar surface while the vehicle was in motion on level or sloping ground. Also, inasmuch as the mission profile was well within the expected capabilities of the Rover and the vehicle was never operated under performance-limiting conditions or under degraded operating modes (except for the front-steering failure during EVA-1), no direct quantitative information exists regarding the limiting mobility-performance capabilities at the Hadley-Apennine region.

The only semiquantitative and qualitative information from the interaction of the vehicle with the lunar surface can be extracted from (1) crew descriptions; (2) photographic coverage of the EVA periods, including a short 16-mm movie taken with the data-acquisition camera while the vehicle was in motion along segments of the EVA-2 traverse; and (3) Rover A-h integrator, odometer, and speedometer read-outs.

Because of the low pressure exerted by the wheels on the lunar soil, caused in part by the light wheel load (approximately 290 N on level terrain) and in part by the wheel flexibility, the average depth of the wheel tracks was only approximately 1-1/4 cm and varied from near zero to 5 cm. High wheel sinkage was usually developed when the vehicle was traversing small fresh craters. On one occasion, because of its light weight, the Rover had the tendency to slide sideways down a rather steep slope as soon as the astronauts stepped off the vehicle. Detailed knowledge of the exact circumstances that led to the tendency of the vehicle to slide downslope may be used to estimate the shear-strength characteristics of the surficial material at that location. Therefore, this particular behavior of the vehicle will be examined further in subsequent analyses.

The 50-percent chevron-covered, wire-mesh Rover wheels developed excellent traction with the lunar surficial material. In most cases, a sharp imprint of the chevron tread was clearly discernible, indicating

that the surficial soil possessed some cohesion and that the amount of wheel slip was minimal. The latter observation is also corroborated by data from the Rover odometer and navigation systems, both of which were calibrated with a constant wheel-slip bias of 2.3 percent. An average wheel sinkage of approximately 1-1/4 cm at a wheel slip of 2.3 percent agrees with the data obtained from Rover wheel-soil interaction tests on lunar-soil simulants performed at the facilities of the U.S. Army Engineers Waterways Experiment Station (WES), Vicksburg, Mississippi, before the mission (ref. 7-13).

In one instance at the ALSEP site, the wheels attained a 100-percent slip while the vehicle was being started. While spinning out, the wheels dug into the lunar soil to a depth of approximately 13 cm (i.e., to the lower part of the wheel rim). The apparent looseness of the soil at this location can be attributed to a local variation in the material consistency, because information relating to the mechanical properties of lunar soil at the ALSEP site (obtained from other sources and discussed in other sections of this report) suggest that the material in this area is, in general, firm.

Driving on previously developed Rover tracks did not materially change the performance of the vehicle, although the LMP commented that, in some instances, the vehicle speed tended to increase. On the basis of crew debriefings and photographic coverage, it appears that the Rover was operated on slopes ranging from 0° to 12°. Because of its light weight and the excellent traction developed by the Rover wire-mesh wheels on the lunar soil, the general performance of the vehicle on these slopes was reported to be satisfactory. On the basis of wheel-soil interaction tests performed on lunar-soil simulants before the mission, the maximum slope angle that could be negotiated by the Rover had been estimated to be approximately 20°. Therefore, it appears that the slopes that were actually negotiated at the Hadley-Apennine region represented, at most, 60 percent of the estimated maximum slope-climbing capability of the vehicle.

Maneuvering the vehicle on slopes did not present any serious problems. It was reported that the vehicle could be controlled more easily upslope than downslope; and, when the vehicle was traversing along slope contours, the wheels on the downslope side tended to displace the soil laterally and to sink a greater amount than the wheels on the upslope side.

This soil behavior again should be interpreted as being local and related to the surficial material rather than to any deep-seated material instability.

Based on crew observations, it appears that no perceptible amount of soil was collected inside the wheel when the vehicle was in motion. This observation is in agreement with the behavior of the lunar-soil simulant used in the WES wheel-soil interaction tests within the range of wheel slip realized during the Rover operation on the lunar surface.

At high vehicle accelerations, a rooster tail was developed by fine-grained material ejected from the wheels. During the performance of the wheel-soil interaction task (Grand Prix), the maximum height of the trajectory of the ejected material was estimated to be 4.5 m. It appears that, because of the presence of the fenders, the material was being ejected forward from the uncovered sides of the wheels. The CDR reported that the ejected dust was below the level of his vision.

In anticipation of local or regional variations in the mechanical properties of the lunar soil traversed by the Rover, extensive wheel-soil interaction studies were performed at the Waterways Experiment Station using a lunar-soil simulant of crushed basalt similar to the one used by Mitchell et al. (ref. 7-3) and Costes et al. (refs. 7-7 and 7-14) for lunar-soil-mechanics simulation studies. For the WES tests, the lunar-soil simulant, designated as LSS (WES mix), had been placed in five consistencies, with the following ranges in properties: specific gravity of solids, 2.69; void ratio, 0.90 to 0.69; and bulk density, 1.52 to 1.71 g/cm<sup>3</sup>.

If the specific gravity of the solid particles of the soil at the Hadley-Apennine area is the same (3.1) as that for the single samples tested from the Apollo 11 and Apollo 12 landing sites, the bulk density of the lunar soil at the same void ratios as those for the LSS (WES mix) would range from 1.63 to 1.83 g/cm<sup>3</sup>. The angle of internal friction of the soil, obtained from triaxial compression tests on air-dry specimens at normal stresses of approximately 0.7 N/cm<sup>2</sup>, ranged between 38.5° and 41.0° (ref. 7-13); cohesion of the soil ranged between 0 and 0.29 N/cm<sup>2</sup>; and the penetration-resistance gradient ranged between 0.2 and 5.9 N/cm<sup>3</sup>. It appears that the range of cohesion and penetration resistance gradient in the soil simulants encompassed the known and calculated range of lunar-soil conditions in the Hadley-Apennine region. Therefore, the apparent agreement between the ob-

served behavior of the Rover on the lunar surface with its expected behavior (based on the WES wheel-soil interaction studies) is an indirect indication of the mechanical properties of the surficial material at the Hadley-Apennine region. More detailed evaluations of Rover wheel-soil interactions at the Apollo 15 site are planned.

## QUANTITATIVE ANALYSES OF SOIL-MECHANICS-TRENCH AND PENETROMETER EXPERIMENTS

Lunar-surface activities unique to the soil-mechanics experiment were conducted at station 8 (fig. 5-2, section 5). From analyses of the soil-mechanics trench and data obtained using the SRP, estimates of the in-place density, cohesion, and angle of internal friction are possible.

### Penetrometer Measurements

The LMP used the SRP for six penetrations—four with the 3.22-cm<sup>2</sup> (base area) cone and two with the 2.54- by 12.70-cm bearing plate. The force-penetration records were scribed on the data drum, which has been returned for analysis.

The penetration curves for tests using the 3.22-cm<sup>2</sup> cone adjacent to the soil-mechanics trench and in a fresh Rover track are shown in figures 7-15(a) and 7-15(b), respectively. It is difficult to determine precisely the depth of penetration from the curves for the other four penetrations because the surface-reference pad of the penetrometer apparently rode up on the shaft during the tests. The surface-reference pad tended to ride up on the shaft when the SRP was vibrated because, although the weight of the reference pad was essentially balanced by the force on the retractor spring, the friction between the reference-pad bushing and the shaft was less than had been anticipated. In each case, however, the stress-penetration curves provide an upper bound on the depth of penetration for an applied force of 111 N, which gives a lower bound on the slope  $G$  of the stress-penetration curve.

The average slope  $G$  of the stress-penetration curve has been correlated with soil porosity, and this correlation can be used to estimate porosity at station 8 from the stress-penetration curves in figure 7-15. The average slope  $G$  was determined (dashed lines in fig. 7-15). Lower bound values of  $G$  were determined



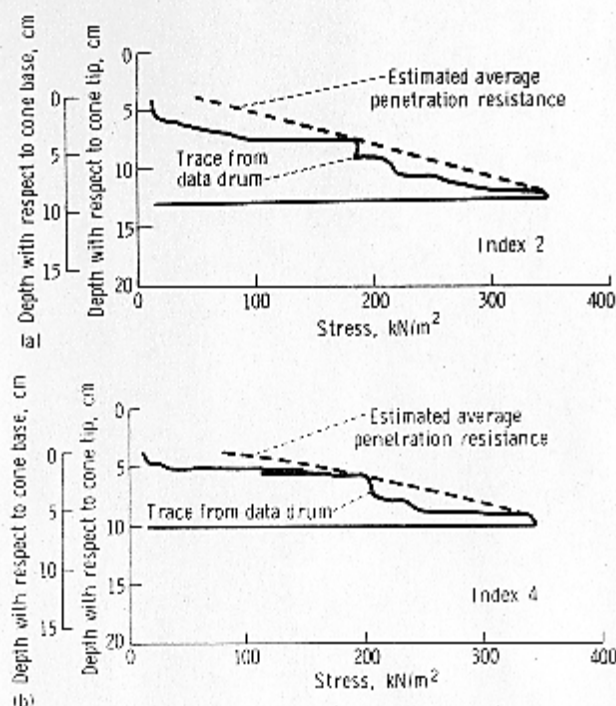


FIGURE 7-15.—Stress compared to penetration records. (a) Adjacent to soil-mechanics trench. (b) In fresh Rover track.

approximately 22 to approximately 16, indicating that the penetrating cone passed into a slightly softer layer below approximately 2 cm. This observation is consistent with a slight compaction of the upper few centimeters under the Rover wheel.

From the data in table 7-III, it appears that a reasonable average value of  $G$  for station 8 in uncompacted soil is approximately 4060 to 4360  $\text{kN/m}^2/\text{m}$ . To compare these values with those obtained on Earth, an account of the effect of gravity must be made. The ratio of  $G$  under terrestrial gravity to  $G$  under lunar gravity for a soil deposit at a given porosity is defined as the gravity-reduction factor. Theoretical and experimental analyses (ref. 7-6) have shown that the gravity-reduction factor ranges from almost 6 for loose soils to approximately 4 for very dense soils. Using the factor for relatively dense soil (behavior of soil from station 8 was characteristic of dense soil), a value of  $G$  that is equivalent to that for the soil at station 8 under terrestrial gravity may be computed to be approximately  $1.6 \times 10^4 \text{ kN/m}^2/\text{m}$  for soil at the same porosity. For soil with a gradation of that of station 8 material, the corresponding porosity ranges from approximately 35 to approximately 38 percent (refs. 7-6, 7-7, and 7-13). To

TABLE 7-III.—Summary of Cone-Penetration-Test Results<sup>a</sup>

Index no.	Location	Penetration at 34 N/cm <sup>2</sup> , cm	Gradient, $G$ , $\text{kN/m}^2/\text{m}$	Penetration depth Base diameter
2	Adjacent to trench	8.25	4060	4.06
3	Bottom of trench	<10.25	>3250	--
4	In Rover track	5.25		2.58
	Upper 2 cm		7590	
	Lower 4 cm		4360	
5	Adjacent to Rover track	<11.25	>2980	--

<sup>a</sup>Cone with base area of 3.22  $\text{cm}^2$ .

similarly from the other two cone tests not shown in figure 7-15. All values are listed in table 7-III.

The data from the SRP test in the Rover track (fig. 7-15(b)) show a slight decrease in slope at a depth of approximately 2 cm (with respect to the base of the cone).<sup>2</sup> The slope decreases from a  $G$ -value of

<sup>2</sup>From independent analyses using soil-cohesion values determined from the soil-mechanics trench and penetrometer data, it was determined that the intercepts at zero penetration with respect to the base of the cone must be no larger than the values shown in figure 7-15.

convert these parameters to density, a value of specific gravity  $G_s$  is required. Because a value of  $G_s$  for Apollo 15 soil has not yet been obtained, the value of 3.1 obtained for single samples of Apollo 11 and 12 soils may be used as an estimate. Porosity, void ratio (ratio of void volume to solid volume), and density for soil with a specific gravity of 3.1 are related in figure 7-16. The estimated range in soil porosity at station 8, as derived from SRP data, is summarized in table 7-IV.

Correlations between porosity and angle of internal friction  $\phi$  have been developed for lunar-soil



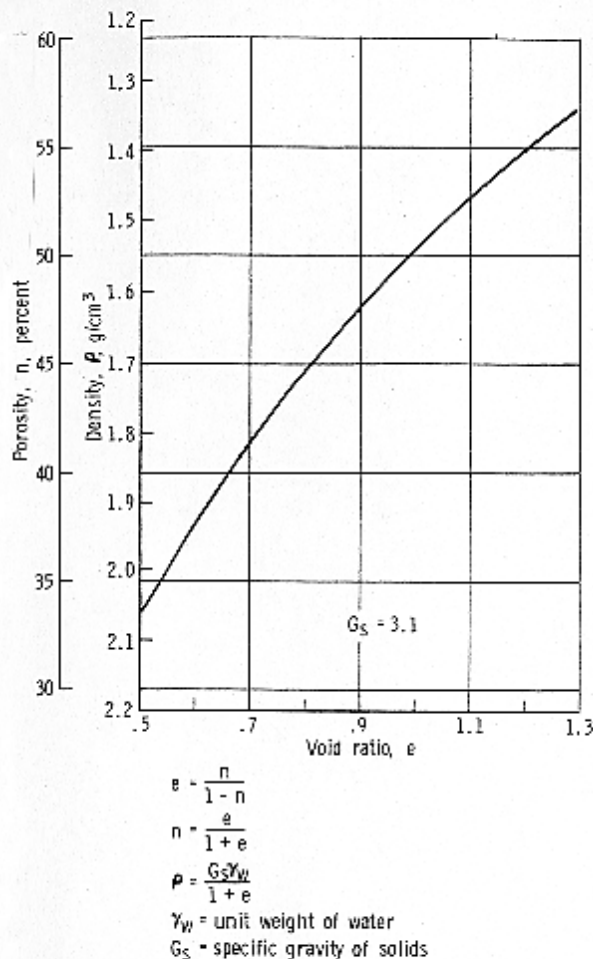


FIGURE 7-16.—Relationships between void ratio, porosity, and density for a soil with a specific gravity of 3.1.

simulants (refs. 7-6, 7-13, and 7-14). From these correlations,  $\phi$  is estimated to be  $49.5^\circ \pm 2^\circ$ .

The estimated densities in table 7-IV are considered appropriate for the upper 10 to 20 cm at station 8. These values are significantly higher than the density of  $1.84 \text{ g/cm}^3$  measured from the uppermost section of the returned drill cores (table 7-II) obtained in the same area. One or more of the

following factors may be responsible for this apparent inconsistency.

(1) The station 8 soil may have a specific gravity significantly less than the assumed value of 3.1. If so, the computed density values in table 7-IV would be lower, although the porosities and void ratios would be unchanged. This question cannot be resolved until specific gravity is measured for Apollo 15 soil.

(2) The drill core may have been loosened during sampling. As a part of the analyses for this report, a series of medium dense to dense deposits of lunar-soil simulant was prepared. Tests on the prepared simulant included driving Apollo 15 prototype core tubes with a hammer. For an initial porosity of approximately 38 percent, no significant change in density was observed during sampling. However, for an initial porosity as low as 35 percent, core-tube studies by Houston and Mitchell (ref. 7-8) indicate that the soil may loosen appreciably during sampling.

(3) Both the estimate of  $1.97 \text{ g/cm}^3$  from the penetration tests and  $1.84 \text{ g/cm}^3$  from the drill core may be correct and reflect local variability.

### Soil-Mechanics Trench

Near the end of EVA-2, the soil-mechanics trench was excavated by the LMP at a point approximately 55 m east-southeast of the ALSEP central station. The lunar surface at the trench site (fig. 7-17) was approximately level except for two small, shallow craters just east of the gnomon. Excavation of the trench was accomplished by using the small scoop attached to the extension handle. Analysis of the television film and commentary by the LMP indicated that excavation proceeded smoothly and without difficulty to a depth reported at the time to be approximately 36 to 41 cm, where a much harder layer was encountered. Subsequent analysis of the television film and the Hasselblad electric data camera photographs has shown that the actual depth was probably somewhat less.

TABLE 7-IV.—Estimated Ranges in Porosity and Friction Angle  $\phi$  for Station 8 Soil as Determined from SRP Data

Value	Porosity, $n$ , percent	Void ratio, $e$	Density, $\rho$ , $\text{g/cm}^3$ (a)	Friction angle, $\phi$ , deg
Best estimate	36.5	0.575	1.97	49.5
Range	35 to 38	0.54 to 0.61	1.92 to 2.01	47.5 to 51.5

<sup>a</sup> $G_s = 3.1$ .

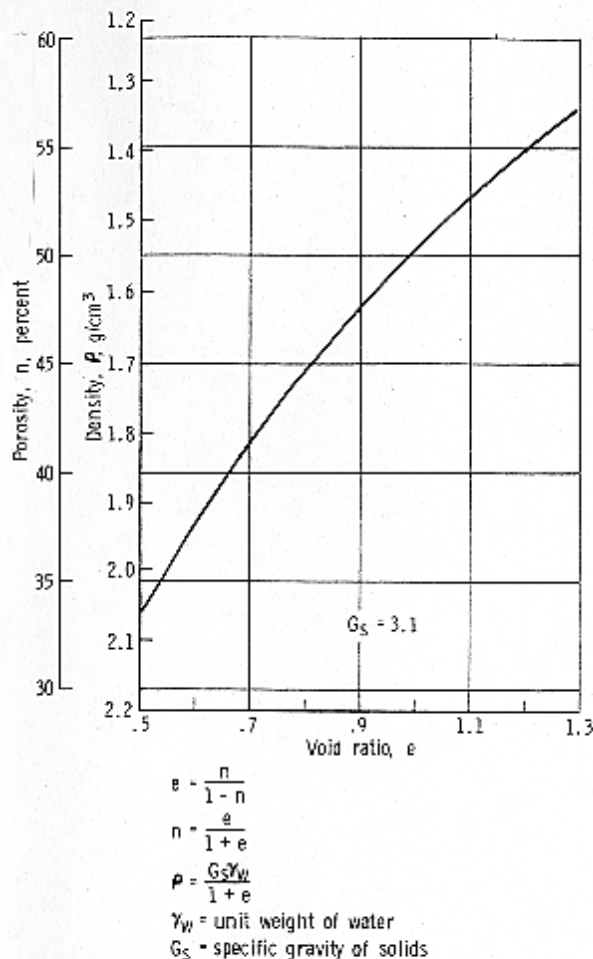


FIGURE 7-16.—Relationships between void ratio, porosity, and density for a soil with a specific gravity of 3.1.

simulants (refs. 7-6, 7-13, and 7-14). From these correlations,  $\phi$  is estimated to be  $49.5^\circ \pm 2^\circ$ .

The estimated densities in table 7-IV are considered appropriate for the upper 10 to 20 cm at station 8. These values are significantly higher than the density of  $1.84 \text{ g/cm}^3$  measured from the uppermost section of the returned drill cores (table 7-II) obtained in the same area. One or more of the

following factors may be responsible for this apparent inconsistency.

(1) The station 8 soil may have a specific gravity significantly less than the assumed value of 3.1. If so, the computed density values in table 7-IV would be lower, although the porosities and void ratios would be unchanged. This question cannot be resolved until specific gravity is measured for Apollo 15 soil.

(2) The drill core may have been loosened during sampling. As a part of the analyses for this report, a series of medium dense to dense deposits of lunar-soil simulant was prepared. Tests on the prepared simulant included driving Apollo 15 prototype core tubes with a hammer. For an initial porosity of approximately 38 percent, no significant change in density was observed during sampling. However, for an initial porosity as low as 35 percent, core-tube studies by Houston and Mitchell (ref. 7-8) indicate that the soil may loosen appreciably during sampling.

(3) Both the estimate of  $1.97 \text{ g/cm}^3$  from the penetration tests and  $1.84 \text{ g/cm}^3$  from the drill core may be correct and reflect local variability.

### Soil-Mechanics Trench

Near the end of EVA-2, the soil-mechanics trench was excavated by the LMP at a point approximately 55 m east-southeast of the ALSEP central station. The lunar surface at the trench site (fig. 7-17) was approximately level except for two small, shallow craters just east of the gnomon. Excavation of the trench was accomplished by using the small scoop attached to the extension handle. Analysis of the television film and commentary by the LMP indicated that excavation proceeded smoothly and without difficulty to a depth reported at the time to be approximately 36 to 41 cm, where a much harder layer was encountered. Subsequent analysis of the television film and the Hasselblad electric data camera photographs has shown that the actual depth was probably somewhat less.

TABLE 7-IV.—Estimated Ranges in Porosity and Friction Angle  $\phi$  for Station 8 Soil as Determined from SRP Data

Value	Porosity, $n$ , percent	Void ratio, $e$	Density, $\rho$ , $\text{g/cm}^3$ (a)	Friction angle, $\phi$ , deg
Best estimate	36.5	0.575	1.97	49.5
Range	35 to 38	0.54 to 0.61	1.92 to 2.01	47.5 to 51.5

<sup>a</sup> $G_s = 3.1$ .

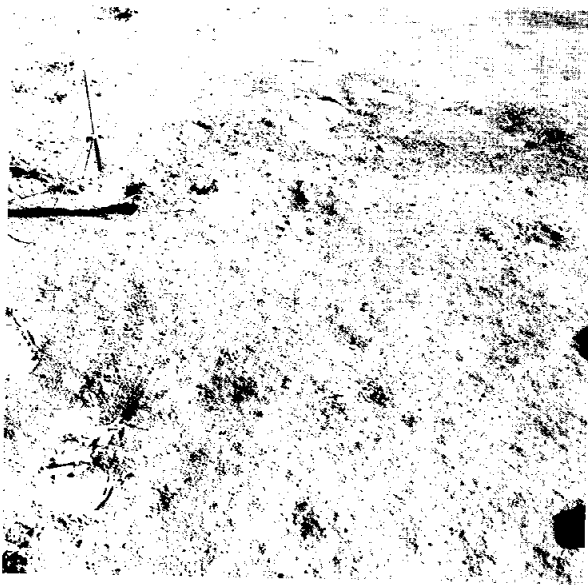


FIGURE 7-17.—Undisturbed lunar surface before excavation of the soil-mechanics trench at station 8. Two small, shallow craters may be seen just to the east of the gnomon (AS15-92-12417).

No evidence exists of layering in the trench wall. The soil was fine grained and cohesive, and a vertical face could be maintained without difficulty. A cross-Sun photograph from the north of the completed trench is shown in figure 7-18. The excavated soil was distributed to the north (foreground of photograph). The smooth scoop marks in the trench wall are evidence of the fineness and cohesiveness of the soil. The footprints in the foreground show the characteristics of recompacted, disturbed material.

The material at the bottom of the trench was reported to be much harder than that above. The LMP indicated that a smooth, flat bottom could be made easily and that further excavation necessitated chipping out the material, which came out in platy fragments approximately 0.5 cm long. However, a sample returned from the trench bottom was dark gray and very cohesive and gave no evidence of hardpan upon examination in the LRL. The cohesion was not destroyed by remolding even after prolonged exposure to an atmosphere. A sample from the top of the trench was similar in behavior to the sample from the bottom, although its grain size was slightly finer (fig. 7-6).

After sampling and photographic documentation of the completed trench, failure of the vertical side wall was induced by loading at the top with the 2.5-

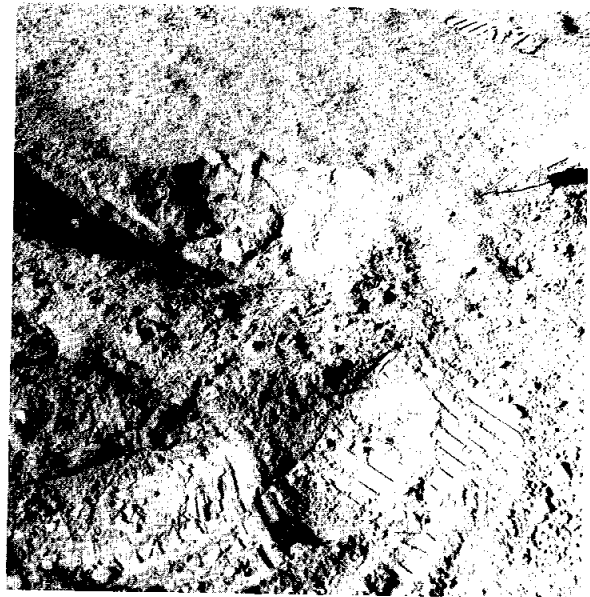


FIGURE 7-18.—Cross-Sun photograph from the north of the completed soil-mechanics trench excavated by the lunar module pilot. Scoop marks on near-vertical face reflect fine-grained, cohesive character of the soil (AS15-92-12440).

by 12.7-cm bearing plate attached to the SRP. The plate was oriented parallel to the trench wall and with the longitudinal center line approximately 10 cm from the top of the trench wall. A cross-Sun view of the failed trench is shown in figure 7-19. The imprint of the lunar reference plane is clearly visible in the photographs. The imprint is 35.6 cm long and 7.9 cm wide.

Detailed photogrammetric analysis of the trench photography is not yet complete. However, sufficiently accurate determination of the trench dimensions has been made to permit some estimates of soil-strength parameters. Failure of the trench wall required the application of a force to the penetrometer bearing plate in excess of the 111-N spring measuring capacity of the SRP. The LMP estimated that he applied an additional 44 N before failure occurred. Collapse was sudden and complete.

It has been shown that the values of soil-strength parameters required for equilibrium of a near-vertical, homogeneous slope are insensitive to the assumed shape of the failure surface (e.g., plane surface of sliding, circular arc, or log spiral). If a planar failure surface is assumed and the shear surfaces at the ends of the failure zone are neglected, the forces and geometry needed for analysis are as shown in figure 7-20.

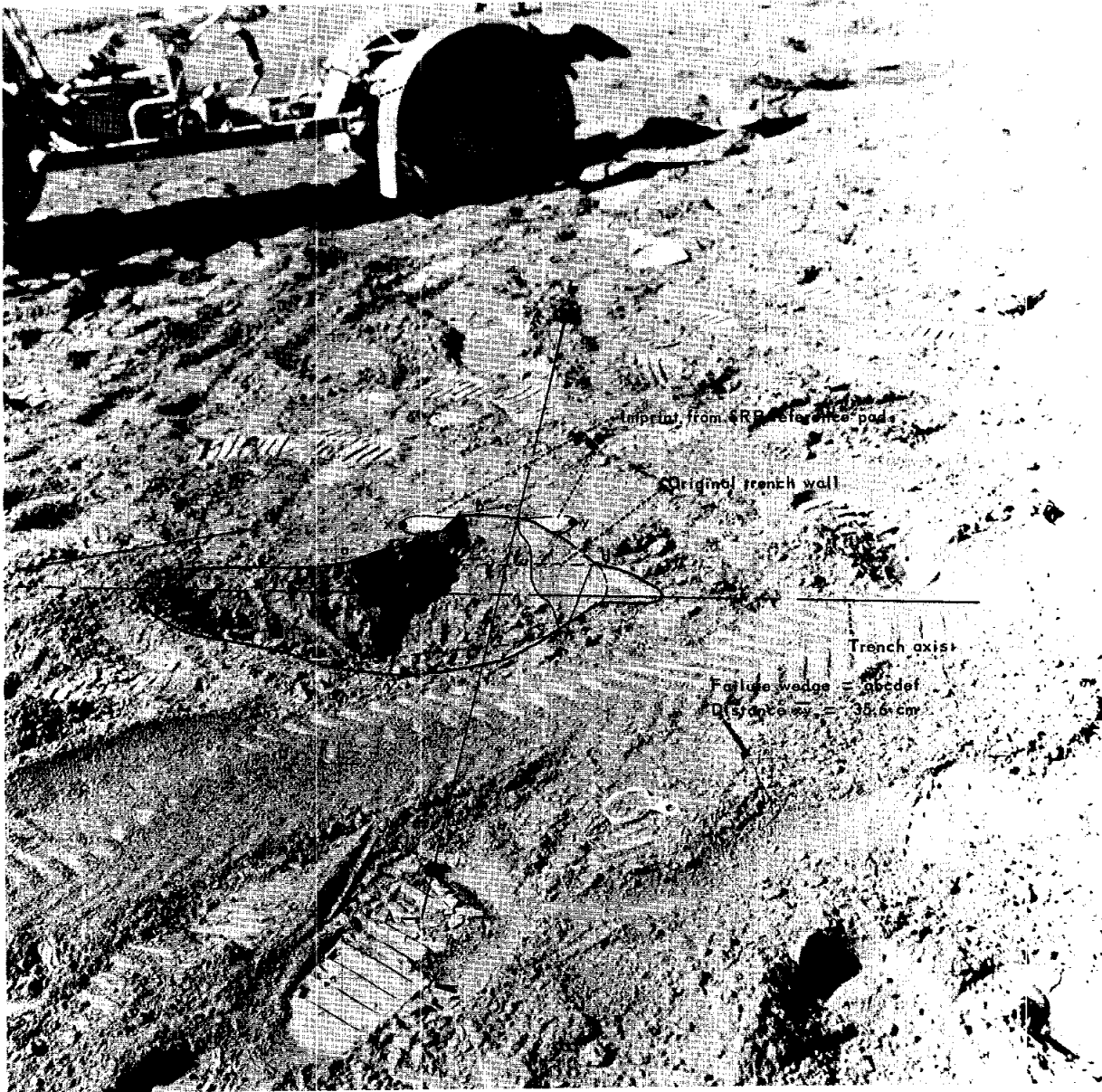


FIGURE 7-19.—Cross-Sun view of soil-mechanics trench at failed vertical wall (AS15-88-11874).

For this case, the analysis is insensitive to the soil unit weight; a density value of  $1.8 \text{ g/cm}^3$  is assumed, which gives a unit weight on the Moon of  $0.00294 \text{ N/cm}^3$ . Equilibrium of the forces shown in figure 7-20 can be expressed in terms of force components parallel to the failure plane; that is

$$F_D = (W_s + 12.25) \cos \left( 45 - \frac{\phi}{2} \right) \quad (7-2)$$

$$F_R = 11.4 \csc \left( 45 - \frac{\phi}{2} \right) c + (W_s + 12.25) \sin \left( 45 - \frac{\phi}{2} \right) \tan \phi \quad (7-3)$$

where

$F_D$  = driving force

$F_R$  = resisting force

$c$  = unit cohesion

$\phi$  = angle of internal friction

$W_s$  = weight of the failure wedge per unit length

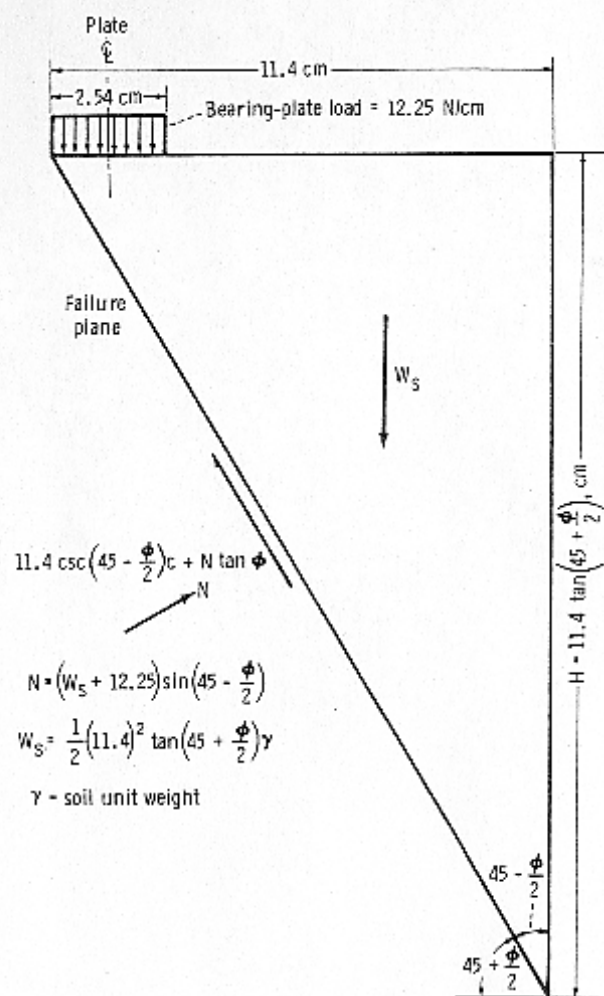


FIGURE 7-20.—Plane-failure analysis of soil-mechanics trench.

After equating  $F_D$  and  $F_R$  and rearranging, the required cohesion may be expressed in terms of the friction angle as

$$c = \frac{W_s + 12.25}{22.8} \left( \frac{1 - \sin \phi}{\cos \phi} \right) \quad (7-4)$$

By the theory of plasticity, this same expression may be derived as an upper bound solution. It may be shown that the selected failure surface is kinematically admissible.

Values of cohesion have been determined as a function of friction angle for the assumed conditions with the results shown in figure 7-21. Also shown in figure 7-21 are the corresponding values of  $H$ , which represent the distance below the top of the trench face at which the failure surface should break out.

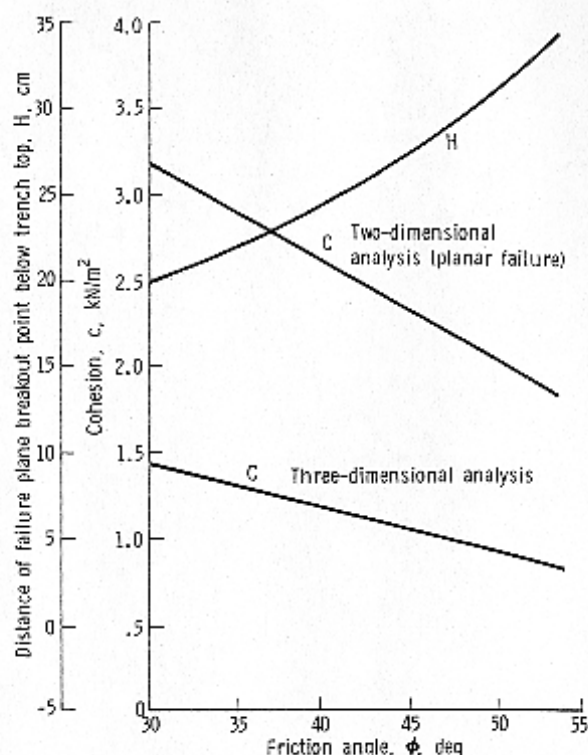


FIGURE 7-21.—Critical values of soil cohesion for trench-wall stability.

Reliable determination of this distance is not possible from the available trench photography; however, the original trench depth appears to be sufficient to accommodate failure in accordance with any of the indicated values of  $\phi$ .

In the analysis that resulted in the cohesion values shown in figure 7-21, end effects were neglected (i.e., plane strain, two-dimensional behavior was assumed). As shown in figure 7-19, the failure wedge involved significant shear areas at the ends. Because of this situation, the values of cohesion shown in figure 7-21 are too high. A preliminary estimate of this shape effect may be made by reducing the computed cohesion values in proportion to the ratio of the area of the assumed planar failure surface to the area of a failure surface that includes the ends of the failure wedge. In the present case, the ratio is computed to be 45 percent for all values of  $\phi$ , resulting in the reduced values of cohesion indicated by the lower curve for cohesion as a function of friction angle in figure 7-21. Although this correction improves the accuracy of the computed cohesion, some uncertainty remains concerning the magnitude of the force required to cause failure. If it is assumed that the LMP's estimate of 44 N more than the 111-N



capacity of the SRP spring is accurate to  $\pm 22$  N, the cohesion values in figure 7-21 will be correct within approximately  $\pm 15$  percent.

Two important features of the trench experiment are that the computed cohesion is not a sensitive function of the friction angle and that the calculation is virtually independent of the value used for soil density. Thus, even when values of friction angle and density are uncertain, the trench experiment provides a reliable basis for determination of soil cohesion.

### Strength Parameters Deduced from Penetration Resistance

One of the most surprising findings at station 8, during measurements with the SRP, was the very high resistance offered by the soil to penetration by the cone with a base area of  $3.22\text{-cm}^2$ . Because of the tendency of the lunar-surface reference plane to ride up on the penetrometer shaft, precise values of penetration are not known for each of the penetration tests, and the exact shape of the curve (force as a function of depth) was not obtained. However, estimates of penetration are possible (table 7-III).

The resistance to penetration  $q_p$  can be calculated by

$$q_p = cN_c\xi_c + \gamma BN_{\gamma q}\xi_{\gamma q} \quad (7-5)$$

where

$c$  = unit cohesion

$\gamma$  = unit weight =  $\rho g$

$B$  = width or diameter of loaded area

$\xi_c, \xi_{\gamma q}$  = shape factors

$N_c, N_{\gamma q}$  = bearing capacity factors =  $f(\phi, \delta/\phi, \alpha, D/B)$

$\phi$  = angle of internal friction

$\delta$  = friction angle between penetrometer cone and soil

$\alpha$  = half the cone apex angle

$\rho$  = density

$D/B$  = ratio of penetration depth to cone diameter

An appropriate penetration-failure mechanism has been assumed for dense soil to enable calculation of the bearing-capacity factors. Durgunoglu<sup>3</sup> has substantiated this failure mechanism by means of model tests and has derived the equations needed for

determination of  $N_{\gamma q}$ ,  $\xi_{\gamma q}$ , and  $N_c\xi_c$ . The value of  $\delta/\phi$  has been taken as 0.55 based on the results of friction measurements between a ground-basalt lunar-soil simulant and hard anodized aluminum similar to that used for the SRP cones. Results from the bearing-capacity equation are insensitive to the value assumed for  $\gamma$ ;  $0.00294\text{ N/cm}^3$  has been assumed here, corresponding to a density  $\rho$  of  $1.8\text{ g/cm}^3$ . Values of  $N_{\gamma q}$ ,  $\xi_{\gamma q}$ , and  $N_c\xi_c$  have been calculated for different values of  $D/B$  and  $\phi$ , and  $q_p = 34.5\text{ N/cm}^2$  (fig. 7-22).

The  $D/B$  ratios for the tests at station 8 fall in the range of approximately 2.5 to 4.1 (table 7-III). Thus, the curve in figure 7-22 for  $D/B = 3$  may represent the actual conditions reasonably well.

The relationship of cohesion compared to friction angle for the trench has been superimposed on figure 7-22. The intersections between this curve and the curves of  $c$  as a function of  $\phi$  for the penetration tests give conditions that can satisfy both trench failure and the penetration test simultaneously. For  $D/B = 3$ , the required cohesion is  $0.94\text{ kN/m}^2$ , and the angle of internal friction is  $51.7^\circ$ . This value compares favorably with that obtained by comparison of the observed penetration behavior with that of the terrestrial simulants (table 7-IV). Although the average friction angle ( $50.6^\circ$ ), computed by the two

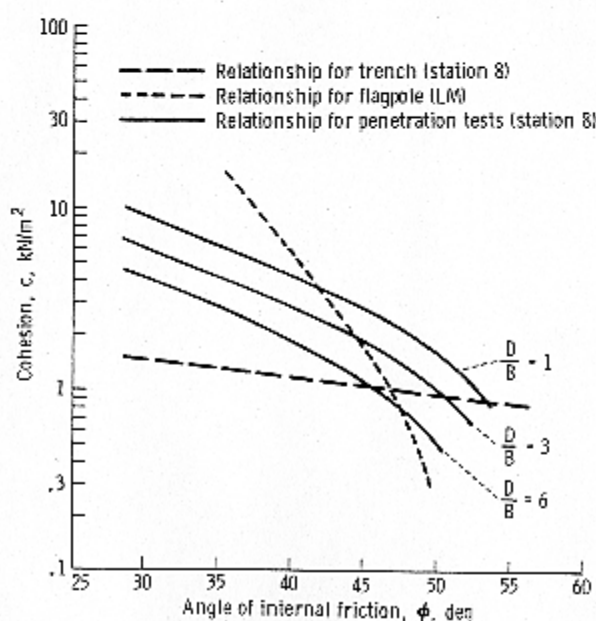


FIGURE 7-22.—Cohesion as a function of friction angle for different penetrations and an 111-N force applied to the SRP.

<sup>3</sup>Durgunoglu, H.T.: Ph. D. dissertation (in preparation). Dept. of Civil Engineering, Univ. of Calif. at Berkeley, 1971.

TABLE 7-V.—Comparison of Estimated Cohesion Values for the Apollo Landing Sites

Mission	Location	Cohesion, kN/m <sup>2</sup>
11	Mare Tranquillitatis	0.35 to 0.70
12	Oceanus Procellarum	0.35 to 0.70
14	Fra Mauro	0.03 to 0.10
15	Hadley-Apennine	0.9 to 1.1

methods, is higher than has been estimated at other Apollo sites, it is consistent with the high soil density at station 8. Similarly, a cohesion of almost 1.0 kN/m<sup>2</sup> is higher than previously measured; but this value, too, can be accounted for by the high density and the relatively fine-grained soil consistency. Table 7-V compares estimates of soil cohesion for the four Apollo landing sites.

A third relationship between  $c$  and  $\phi$  may be deduced from the penetration of the flagpole into the soil near the LM. The flagpole, made of chrome-anodized aluminum, is a hollow tube with an outside diameter of 2.226 cm and a wall thickness of 0.089 cm. From study of the television tapes, it was deduced that the 119.05-cm-long lower section of the pole was pushed to a depth of approximately 51 cm before requiring hammering. The LMP was observed to apply his full weight to the pole because both feet were off the ground simultaneously. His suited weight in the lunar gravity field is approximately 27 kg.

The force of penetration  $F$  is resisted by end bearing and skin friction according to

$$F = q_p A_p + f_s A_s \quad (7-6)$$

where

$$q_p = \text{unit end-bearing capacity} = cN_c \xi_c + \gamma BN \gamma_q \xi_{\gamma q}$$

$A_p$  = end-bearing area  
 $A_s$  = surface area in contact with the soil  
 $f_s$  = unit skin friction

If the unit skin friction is assumed to increase linearly from zero at the ground surface to a maximum at the bottom of the pole, depth  $D$ , then  $f_s$  is given by

$$f_s = \frac{\gamma DK \tan \delta}{2} \quad (7-7)$$

where  $K$  is the coefficient of lateral Earth pressure

$\cong 0.5$ , and  $\tan \delta$  is the friction coefficient between soil and pole  $\cong 0.5$ .

With the aid of these relationships and the assumption that the flagpole behaved in a manner similar to that of the core tubes and did not plug during penetration, values of  $c$  have been computed and plotted on figure 7-22 as a function of  $\phi$ . This relationship defines smaller values for  $c$  and  $\phi$  than are required to satisfy the behavior at station 8. This difference could be attributed to a lower soil density at the flagpole location. From examination of the LM and photographs (e.g., fig. 7-11) it is assumed that this may be the case. The flagpole appears to have been placed in the rim of a small crater, and the soil at small crater rims is generally softer than in intercrater regions.

## DISCUSSION

### Lunar-Soil Density

The bulk density of the lunar soil has been the subject of speculation since early in the lunar-exploration program. Table 7-VI summarizes some of the estimates that have been made since that time.

A density of 0.3 g/cm<sup>3</sup> (corresponding to a porosity of 90 percent) was assumed by Jaffe (refs. 7-15 and 7-16) in an effort to calculate lower bound bearing capacities for the design of unmanned and manned lunar-landing craft. Halajian (ref. 7-17) also used a very low density, 0.4 g/cm<sup>3</sup>, but believed that the strength of the lunar surface was similar to that of pumice. The grain-size distribution and the lunar-soil/footpad interaction observed on Surveyor I (June 1966) suggested a value of 1.5 g/cm<sup>3</sup> (ref. 7-18). In December 1966, the Russian probe, Luna 13, provided the first in-place measurement of soil density on the Moon by means of a gamma-ray device. Unfortunately, the calibration curve for this device was double valued, and it was necessary to choose between a value of 0.8 and 2.1 g/cm<sup>3</sup>. Cherkasov et al. (ref. 7-19) chose the lesser value. Based on the results from the soil-mechanics surface-sampler experiments on Surveyors III and VII, Scott and Roberson (refs. 7-5 and 7-20) confirmed the Surveyor I value of 1.5 g/cm<sup>3</sup> and argued (ref. 7-21) that the Russian investigators had chosen the wrong portion of their calibration curve.

Ironically, the drive-tube data from Apollo 11 also were ambiguous, because of the shape of the bit. The

TABLE 7-VI.—*Estimates of Lunar-Soil Density*

<i>Bulk density, <math>\rho</math>, g/cm<sup>3</sup></i>	<i>Investigator</i>	<i>Landing site</i>	<i>Reference</i>
0.3	Jaffe	--	7-15 and 7-16
0.4	Halajian	--	7-17
1.5	Christensen et al.	Surveyor I	7-18
0.8	Cherkasov et al.	Luna 13	7-19
1.5	Scott and Roberson, and Scott	Surveyors III and VII	7-20, 7-5, and 7-21
1.54 to 1.75	Costes and Mitchell	Apollo 11	7-22
0.75 to >1.75	Scott et al.	Apollo 11	7-23
<sup>a</sup> 1.81 to 1.92	Costes et al.	Apollo 11	7-7
1.6 to 2.0	Scott et al.	Apollo 12	7-23
<sup>a</sup> 1.80 to 1.84	Costes et al.	Apollo 12	7-7
1.55 to 1.90	Houston and Mitchell	Apollo 12	7-8
1.7 to 1.9	Carrier et al.	Apollo 12	7-9
1.2	Vinogradov	Luna 16	7-24
1.35 to 2.15	Mitchell et al.	Apollo 15	(b)

<sup>a</sup>Upper bound estimates.<sup>b</sup>This report.

bulk densities of the soil in the two core tubes were 1.59 and 1.71 g/cm<sup>3</sup> (ref. 7-1) or 1.54 and 1.75 g/cm<sup>3</sup> as later reported by Costes and Mitchell (ref. 7-22) by taking into account possible differences in core-tube diameter. These densities could have indicated an in situ density from 0.75 g/cm<sup>3</sup> to more than 1.75 g/cm<sup>3</sup> (ref. 7-23).

The shape of the Apollo 12 drive-tube bits reduced the uncertainty, and the density at this site was estimated to be 1.6 to 2.0 g/cm<sup>3</sup> (ref. 7-23). Core-tube simulations performed later by Houston and Mitchell (ref. 7-8) and Carrier et al. (ref. 7-9) yielded additional estimates of 1.55 to 1.90 g/cm<sup>3</sup> and 1.7 to 1.9 g/cm<sup>3</sup>, respectively. Based on penetration-resistance data from the Apollo 11 and 12 landing sites, Costes et al. (ref. 7-7) gave upper bound estimates of the density at the two sites of 1.8 to 1.94 g/cm<sup>3</sup> and 1.81 to 1.84 g/cm<sup>3</sup>, respectively. Vinogradov (ref. 7-24) estimated a value of 1.2 g/cm<sup>3</sup> from a rotary-drill sample returned by Luna 16.

*Density of the lunar soil at the Apollo 15 site.*—The early estimates of lunar-soil density were intended as lower bounds for the entire lunar surface. When returned core-tube samples became available, it was possible to estimate a range of densities for a given landing site. The new core tubes on Apollo 15 have permitted estimates of the in situ density for different locations within the site.

The density at each of the drive-tube locations is

estimated by correcting the bulk density in the tubes for disturbance caused by sampling. These corrections must await detailed core-tube-simulation studies, which will be performed later. In the meantime, the high percent core recoveries (table 7-II) suggest that the corrections will be small, and a preliminary estimate can be made of density as opposed to depth at the three core-tube locations (fig. 7-23). The top 25 to 35 cm of soil along the Apennine Front (stations 2 and 6) have very similar, low average values of density, ~1.35 g/cm<sup>3</sup>. The soil density evidently increases rapidly with depth. The soil density measured at the Apennine Front is approximately 10 percent less than the density at any previous Surveyor or Apollo site and approaches that of the Luna 16 site (1.2 g/cm<sup>3</sup>). The average soil density at Hadley Rille (station 9A) is significantly higher in the top 30 cm (~1.69 g/cm<sup>3</sup>) and increases less rapidly with depth. If the density is assumed to increase linearly with depth, the station 2 data would yield a density of 1.2 g/cm<sup>3</sup> at the surface, increasing to 1.8 g/cm<sup>3</sup> at a depth of 63 cm. The station 9A data would yield a value of 1.6 g/cm<sup>3</sup> at the surface (33 percent higher than at station 2) and 1.9 g/cm<sup>3</sup> at a depth of 64 cm. Densitometric analyses of the X-radiographs are planned in an effort to develop detailed relationships of density as a function of depth for the Apollo 15 core tubes.

The in situ density at the soil-mechanics trench,



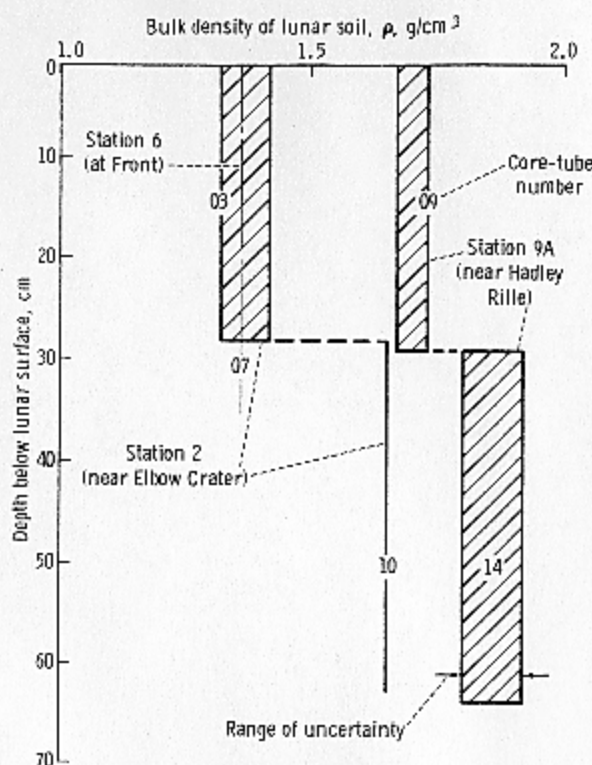


FIGURE 7-23.—Preliminary density compared to depth estimates at the three Apollo 15 core-tube sites.

station 8, has been estimated to be in the range of 1.92 to 2.01 g/cm<sup>3</sup>, based on the penetration test results. The data in table 7-II indicate a density range of 1.62 to 2.15 g/cm<sup>3</sup> for the samples in the deep drill stem obtained from the same area. Average density of these samples is approximately 1.8 g/cm<sup>3</sup>. Possible explanations for the differences according to the two methods have been discussed in the subsection entitled "Penetrometer Measurements." Because significant variations in density exist both regionally and locally on the lunar surface, further study is required to relate these differences in a consistent manner to surface-material composition, history, and lunar processes.

**Relative and absolute density.**—Now that more accurate values of the absolute density of lunar-soil deposits are becoming available, it is important that the relative density be determined, because mechanical properties are strongly dependent on relative density as well as on absolute density and porosity.

Relative density  $D_R$  is defined by

$$D_R = \frac{e_{\max} - e}{e_{\max} - e_{\min}} \times 100 \text{ percent} \quad (7-8)$$

where

$e_{\max}$  = maximum void ratio (corresponding to minimum density) at which the soil deposit can exist

$e_{\min}$  = minimum void ratio (corresponding to maximum density) at which the soil deposit can exist

It can be shown easily that relative density can also be calculated in terms of bulk density according to

$$D_R = \frac{\rho_{\max}}{\rho} \frac{\rho - \rho_{\min}}{\rho_{\max} - \rho_{\min}} \times 100 \text{ percent} \quad (7-9)$$

If  $\rho = \rho_{\min}$  (or  $e = e_{\max}$ ),  $D_R = 0$  percent and the deposit is exceptionally loose; if  $\rho = \rho_{\max}$  (or  $e = e_{\min}$ ),  $D_R = 100$  percent and the soil is very compact.

Compressibility, disturbance during sampling, penetration resistance, and shear strength are far more dependent on the relative density than on the absolute density of a given soil deposit. Because  $\rho_{\max}$  and  $\rho_{\min}$  can vary from soil to soil (depending primarily on the specific gravity, grain-size distribution, grain-shape distribution, and particle surface texture), different deposits can have different absolute densities but similar relative densities. The behavior of such deposits would then be similar. It is also possible to have similar absolute densities and quite different relative densities, and this will result in significantly different behavior. The lunar soils at the Apollo 15 site have been deposited at different absolute and relative densities. Determination of the relative densities would contribute significantly to the evaluation of the data from many experiments. Until determinations of specific gravity and minimum and maximum density are made on returned lunar samples, definitive conclusions are difficult to reach.

### Penetrability Considerations

Penetration of the lunar surface for purposes of measuring in situ properties, obtaining core-tube samples, or emplacing probes (as in the heat-flow experiment (HFE)) may be limited by the presence of

obstructing large particles or by excessive penetration resistance. A probability analysis was made to determine the likelihood that the three core tubes, four cone penetrations, two heat-flow drill holes, and the deep core could be made to their respective depths without encountering an obstructing particle or rock fragment. The method of analysis has been described previously by Mitchell et al. (ref. 7-4). The Apollo 12 size-frequency distribution curve was used for this preliminary analysis because complete Apollo 14 and Apollo 15 size-frequency distribution curves are not yet available.

The analysis indicated a probability of 0.9 that the four cone-penetration tests would reach their respective depths without striking a particle equal to or larger than the cone diameter of 2.03 cm. The probability that the three core tubes could be driven to their respective depths without striking a particle equal to or larger than the tube diameter (4.39 cm) was 0.75. From another analysis, also based on Apollo 12 particle-size distributions, it was predicted that the chance of the core-tube material containing one particle of approximately 1.3-cm diameter is approximately 50 percent. The probability of finding a rock between 2 and 4 cm in the core tubes is only 0.2. In actuality, the Apollo 15 cores contain several rock fragments in the 1.3-cm size range, and the double-core-tube sample taken at station 9A near Hadley Rille contained a rock fragment 2.2 by 2.6 by 4.8 cm near the bottom of the core.

The probability that the HFE drill core would reach full depth (2.36 m) without striking a fragment equal to or greater than the outside diameter of the drill (2.62 cm) was 0.6. The probability that both HFE holes would reach depths of 178 and 175 cm, respectively, without striking a particle equal to or greater than the drill bit diameter (2.856 cm) was 0.5. If the HFE holes had reached full design depth of 3 m, the calculated probability is 0.7 that a particle greater than or equal to the drill diameter would be encountered and 0.5 that a particle more than twice the drill diameter would be encountered.

In areas of high density, penetration to depths of more than a few centimeters using a penetrometer or core tube may not be possible without mechanical assistance (e.g., drill or jack) to aid the astronaut. To investigate this possibility, a soil simulant was prepared to provide behavior comparable to that observed at station 8, and penetration and core-tube-sampling studies were made. For the soil simulant,

the stress-penetration curves obtained were very similar in shape, slope  $G$ , and appearance to those obtained at station 8.

It was necessary to make the porosity of the simulant greater than that estimated for the lunar soil at station 8 to account for the effect of gravity. Because the resistance to penetration with the SRP was essentially the same, quantitatively, for the lunar soil as for the simulant, it is reasonable to conclude that the resistance to core-tube penetration would also be similar. Two separate core tubes similar to those used on Apollo 15 were first pushed and then hammered to the depth of a single core tube. For an applied vertical static force of approximately 245 N, the average depth of penetration was approximately 10 cm. A total of 60 blows with a hammer similar to that used on Apollo 15 were then required to drive the tube the rest of the way.

These data indicate that considerable difficulty would have been encountered in obtaining a single-core-tube sample at station 8 if it had been attempted. Driving a double core tube probably would have been impossible. Thus, it appears from these studies that if the total depth of penetration with the SRP using the 3.22-cm<sup>2</sup> cone is approximately 7.5 cm or less, core-tube sampling may not be practical.

### Core-Tube and Borehole Stability

Figure 7-10 shows open holes that remained after removal of the core tubes from the ground. The crewmen reported that the deep drill hole also remained open after the drill stem was removed. Some soil cohesion is required to prevent collapse of the holes, and a simplified analysis of this condition is possible using the theory of elasticity. The maximum principal stress difference  $(\sigma_\theta - \sigma_r)_{\max}$  is at the surface of the hole, where radial stress  $\sigma_r$  is zero, and tangential stress  $\sigma_\theta$  equals  $2p$ , where  $p$  is the lateral pressure in the ground away from the zone of influence of the hole. If the soil adjacent to the hole is disturbed or yields, a plastic zone will form around the hole; however, it may be shown (ref. 7-25) that the maximum shear stress in the zone will be less than that for the purely elastic case. Determination of values of  $c$  and  $\phi$  to withstand the maximum applied

shear stress  $\tau_{\max} = \frac{(\sigma_\theta - \sigma_r)_{\max}}{2}$  will enable determination of the depth to which stresses will be elastic. The appropriate equation is

$$c = p \left( \frac{1 - \sin \phi}{\cos \phi} \right) = \frac{\nu}{1 - \nu} \rho g z \left( \frac{1 - \sin \phi}{\cos \phi} \right) \quad (7-10)$$

where  $\nu$  is Poisson's ratio,  $g$  is acceleration caused by gravity, and  $z$  is depth of elastic zone.

For a Poisson's ratio of 1/3 (which corresponds to an Earth pressure coefficient of 0.5) and a density of 1.8 g/cm<sup>3</sup>, the relationship between  $c$ ,  $\phi$ , and depth of elastic zone is as shown in figure 7-24. Below this depth, a plastic zone will exist extending to a distance  $r_e$  from the centerline of the hole. For any finite values of  $c$  and  $z$ , the value of  $r_e$  is finite, and a failure of the walls should not occur. However, as the hole becomes deep and the plastic zone becomes large, extensive lateral straining of the soil may occur, eventually causing a closure of the hole by inward squeezing of the soil. This phenomenon would not be expected to occur for the relatively shallow depths being drilled on the lunar surface and for the values of cohesion and friction angle that have been determined.

### CONCLUSIONS

More extensive opportunities for detailed study of the mechanical properties of lunar soil have been provided by the Apollo 15 mission than by previous missions; and, for the first time in the Apollo Program, quantitative measurement of forces of interaction between a soil-testing device and the lunar surface has been possible. Preliminary conclusions can be drawn from the analyses completed to date.

(1) The lunar surface of the Hadley-Apennine site is similar in color, texture, and general behavior to that at the previous Apollo sites.

(2) Variability between grain-size distributions of different samples from the Apollo 15 site does not appear to be as great as at the Apollo 12 and 14 sites.

(3) Considerable variability exists in soil properties, as reflected by density, strength, and compressibility, both with depth and laterally. Lateral variations are both regional (as characterized by conditions ranging from soft, compressible soil along the Apennine Front to firmer, relatively incompressible soil near the rim of Hadley Rille) and local as can be observed from variable footprint depths visible in many photographs.

(4) Through the use of new core-tubes, designed on the basis of soil-mechanics considerations and used for the first time on the Apollo 15 mission, 3302 g of

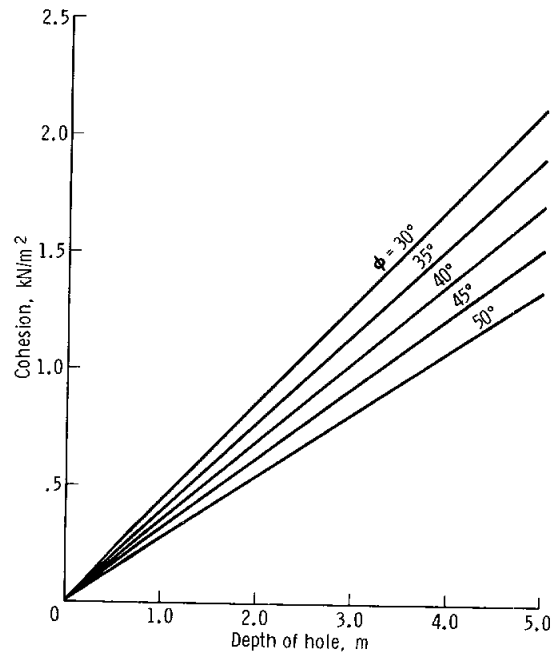


FIGURE 7-24.—Depth to bottom of elastic zone in an open bore hole.

relatively undisturbed lunar soil were returned. The performance of these tubes was excellent.

(5) In situ soil densities that were deduced from the core-tube and drill-stem samples vary considerably (from 1.36 to 2.15 g/cm<sup>3</sup>). These results reinforce the evidence for soil variability available from other sources (e.g., photography and crew commentary).

(6) No evidence exists of past deep-seated slope failures, although the surface material may be in a near-failure condition along the Apennine Front, and there is evidence of the downslope movement of surficial material on the Hadley Rille walls.

(7) Blowing dust caused greater visibility degradation during LM landing than in previous missions. This situation may be related to the descent path, vertical velocity, Sun angle, and local soil conditions.

(8) Limited amounts of quantitative data are available on Rover-soil interaction. The apparent agreement between the observed Rover behavior on the lunar surface and the expected behavior, based on premission simulation studies, provides an indirect measure of the mechanical properties of the surficial soil in the Hadley-Apennine region.

(9) The SRP, used for the first time on this mission, has provided quantitative information on the penetration resistance of the lunar surface. Penetration data obtained at station 8 have indicated a soil of high density ( $1.97 \text{ g/cm}^3$ ), high strength, and low compressibility. Both theoretical analyses and the behavior of terrestrial simulants indicate an angle of internal friction at this site of approximately  $50^\circ$ . This high value is consistent with the high density.

(10) Analysis of the soil-mechanics trench-wall failure and the SRP data lead to an estimate for soil cohesion at station 8 of approximately  $1.0 \text{ kN/m}^2$ . This represents a cohesion greater than that apparent at the Apollo 11, 12, and 14 sites. This cohesion would be expected on the basis of the fine grain size and high density.

(11) A consideration of the variability of soil density on the lunar surface in conjunction with the strong dependence of other properties (strength and compressibility) on density, porosity, and relative density reinforces the need for determinations of the specific gravity and maximum and minimum densities for lunar-soil samples, if proper interpretation of lunar-soil behavior is to be made.

(12) The results of terrestrial simulations have indicated that it is unlikely that a core tube could have been pushed or hammered to its full length into the lunar surface at station 8. The data provide a basis for estimating the feasibility of core-tube sampling from the depth of penetration obtainable using the SRP.

(13) The stability of open core-tube holes and boreholes on the lunar surface has been analyzed, and collapse would not be expected for the shallow depths being drilled.

(14) The methods used to obtain soil-mechanics data have worked well, with the exception of the tendency of the SRP reference plane to ride up (which can be corrected easily). The quantitative values for soil properties deduced from the test results are considered reliable. The close correspondence between properties deduced using simulants and from theoretical analyses is particularly significant.

(15) Additional analyses are needed to relate the properties of lunar soil deduced herein and the variability of such properties to compositional and geological conditions on the lunar surface and to the processes that have shaped their history.

## REFERENCES

- 7-1. Costes, N.C.; Carrier, W.D.; Mitchell, J.K.; and Scott, R.F.: Apollo 11 Soil Mechanics Investigation. Sec. 4 of Apollo 11 Preliminary Science Report, NASA SP-214, 1969.
- 7-2. Scott, R.F.; Carrier, W.D.; Costes, N.C.; and Mitchell, J.K.: Mechanical Properties of the Lunar Regolith. Sec. 10 of Apollo 12 Preliminary Science Report, Part C, NASA SP-235, 1970.
- 7-3. Mitchell, J.K.; Houston, W.N.; Vinson, T.S.; Durgunoglu, T.; et al.: Lunar Surface Engineering Properties and Stabilization of Lunar Soils. Univ. of Calif. at Berkeley, Space Sciences Laboratory, NASA Contract NAS 8-21432, 1971.
- 7-4. Mitchell, J.K.; Bromwell, L.G.; Carrier, W.D.; Costes, N.C.; and Scott, R.F.: Soil Mechanics Experiment. Sec. 4 of Apollo 14 Preliminary Science Report, NASA SP-272, 1971.
- 7-5. Scott, R.F.; and Roberson, F.I.: Soil Mechanics Surface Sampler. Surveyor Project Final Report, Part II: Science Results, Technical Report 32-1265, JPL, Pasadena, Calif., June 15, 1968, pp. 195-206.
- 7-6. Houston, W.N.; and Namiq, L.I.: Penetration Resistance of Lunar Soils. *J. Terramechanics*, vol. 8, no. 1, 1971, pp. 59-69.
- 7-7. Costes, N.C.; Cohron, G.T.; and Moss, D.C.: Cone Penetration Resistance Test—An Approach to Evaluating the In-Place Strength and Packing Characteristics of Lunar Soils. Proceedings of the Second Lunar Science Conference, vol. 3, A.A. Levinson, ed., Pergamon Press (Cambridge, Mass.), 1971, pp. 1973-1987.
- 7-8. Houston, W.N.; and Mitchell, J.K.: Lunar Core Tube Sampling. Proceedings of the Second Lunar Science Conference, vol. 3, A.A. Levinson, ed., MIT Press (Cambridge, Mass.), 1971, pp. 1953-1958.
- 7-9. Carrier, W.D., III; Johnson, S.W.; Werner, R.A.; and Schmidt, R.: Disturbance in Samples Recovered with the Apollo Core Tubes. Proceedings of the Second Lunar Science Conference, vol. 3, A.A. Levinson, ed., MIT Press (Cambridge, Mass.), 1971, pp. 1959-1972.
- 7-10. Scott, R.F.: Principles of Soil Mechanics. Addison-Wesley (Reading, Mass.), 1963.
- 7-11. Lunar Sample Preliminary Examination Team: Preliminary Examination of Lunar Samples from Apollo 14. *Science*, vol. 173, no. 3998, Aug. 20, 1971, pp. 581-693.
- 7-12. Lindsay, J.F.: Sedimentology of Apollo 11 and 12 Lunar Soils. *J. Sed. Petr.*, Sept. 1971.
- 7-13. Green, A.J.; and Melzer, K.J.: Performance of Boeing-GM Wheels in a Lunar Soil Simulant (Basalt). Tech. Rept. M-70-15, USAE WES, Vicksburg, Miss., 1970.
- 7-14. Costes, N.C.; et al.: Lunar Soil Simulation Studies in Support of the Apollo 11 Mission. Geotechnical Research Laboratory, Space Sciences Laboratory, Marshall Space Flight Center, Huntsville, Ala., 1969.
- 7-15. Jaffe, Leonard D.: Depth and Strength of the Lunar Dust. *Trans. Amer. Geophys. Union*, vol. 45, Dec. 30, 1964, p. 628.

- 7-16. Jaffe, Leonard D.: Strength of the Lunar Dust. *J. Geophys. Res.*, vol. 70, no. 24, Dec. 15, 1965, pp. 6139-6146.
- 7-17. Halajian, J.D.: The Case for a Cohesive Lunar Surface Model. Report ADR 04-40-64.2, Grumman Aircraft Engineering Corp., Research Dept., Bethpage, New York, June 1964.
- 7-18. Christensen, E.M.; Batterson, S.A.; Benson, H.E.; Chandler, C.E.; et al.: Lunar Surface Mechanical Properties. Surveyor I Mission Report, Part II: Scientific Data and Results, Technical Report 32-1023, JPL, Pasadena, Calif., Sept. 10, 1966, pp. 69-85.
- 7-19. Cherkasov, I.I.; Vakhnin, V.M.; Kemurjian, A.L.; Mikhailov, L.N.; et al.: Physical and Mechanical Properties of the Lunar Surface Layer by Means of Luna 13 Automatic Station. *Moon and Planets II*, A. Dollfus, ed., North-Holland Pub. Co. (Amsterdam), 1968, pp. 70-76.
- 7-20. Scott, R.F.; and Roberson, F.I.: Soil Mechanics Surface Sampler: Lunar Tests, Results, and Analyses. Surveyor III Mission Report, Part II: Scientific Data and Results, Tech. Rept. 32-1177, JPL, Pasadena, Calif., June 1, 1967, pp. 69-110.
- 7-21. Scott, R.F.: The Density of the Lunar Surface Soil. *J. Geophys. Res.*, vol. 73, no. 16, Aug. 15, 1968, pp. 5469-5471.
- 7-22. Costes, N.C.; and Mitchell, J.K.: Apollo 11 Soil Mechanics Investigation. Proceedings of the Apollo 11 Lunar Science Conference, vol. 3, A.A. Levinson, ed., Pergamon Press (New York), 1970, pp. 2025-2044.
- 7-23. Scott, R.F.; Carrier, W.D., III; Costes, N.C.; and Mitchell, J.K.: Apollo 12 Soil Mechanics Investigation. *Geotechnique*, vol. 21, no. 1, Mar. 1971, pp. 1-14.
- 7-24. Vinogradov, A.P.: Preliminary Data on Lunar Ground Brought to Earth by Automatic Probe "Luna-16." Proceedings of the Second Lunar Science Conference, vol. 1, A.A. Levinson, ed., MIT Press (Cambridge, Mass.), 1971, pp. 1-16.
- 7-25. Obert, L.; and Duvall, W.I.: Rock Mechanics and the Design of Structure in Rock. John Wiley & Sons, Inc. (New York), 1967.

## ACKNOWLEDGMENTS

The assistance of the individuals who have contributed to the preparation for, execution of, and data analysis from the soil-mechanics experiment is gratefully acknowledged. In particular, the authors wish to express appreciation to Astronauts David R. Scott and James B. Irwin, who were able to complete the station 8 soil-mechanics activities in an excellent manner despite a greatly compressed time line.

The basic design concept of the SRP was developed at the Geotechnical Research Laboratory of the NASA Marshall Space Flight Center Space Sciences Laboratory with the support of Teledyne-Brown Engineering Company, Huntsville, Alabama. Dr. Rolland G. Sturm, Roland H. Norton, George E. Campbell, and G.T. Cohron were instrumental in the development of this concept. The final design, construction, and qualification of the flight article were carried through by W.N. Dunaway and W. Lyon of the NASA Manned Spacecraft Center and W. Young of the General Electric Company.

Dr. H. John Hovland, L.I. Namiq, H. Turan Durgunoglu, Donald D. Treadwell, and Y. Moriwaki, all of the soil-mechanics research staff at the University of California, were responsible for many of the simulation studies, data analyses, and computations discussed in this report.

Dr. Stewart W. Johnson, National Research Council Senior Postdoctoral Fellow from the Air Force Institute of Technology, and Richard A. Werner, Lisimaco Carrasco, and Ralf Schmidt of Lockheed Electronics Company participated in work at the Manned Spacecraft Center.

Fred W. Johnson participated in the probability analyses and photographic studies done at the Massachusetts Institute of Technology.